Doctor of philosophy

Inhibitory molecular mechanisms of inflammatory and Hormonal deficiency- induced bone loss

The Graduate School of the University of Ulsan

Department of Biological Sciences

Inhibitory molecular mechanisms of inflammatory and Hormonal deficiency- induced bone loss

Supervisor: Hye-Seon Choi

A Dissertation

Submitted to the graduate School of the University of Ulsan

In partial Fulfillment of the Requirements for the Degree

Doctor of philosophy

By

Malihatosadat Gholam Zadeh

August 2022

Doctor of philosophy

Inhibitory molecular mechanisms of inflammatory and Hormonal deficiency- induced bone loss

This certifies that the dissertation

of Malihatosadat Gholam Zadeh is approved.

Committee Chair Dr. Mann Kyoon Shin

Committee Member Dr. Jeong-Woo Park

Committee Member Dr. Hye-Seon Choi

Committee Member Dr. Kim Hongpyo

Committee Member Dr. Kim Jae-geun

Department of Biological Sciences

Ulsan, Korea

August 2022

Doctor of philosophy

Inhibitory molecular mechanisms of inflammatory and Hormonal deficiency- induced bone loss

This certifies that the dissertation

of Malihatosadat Gholam Zadeh is approved

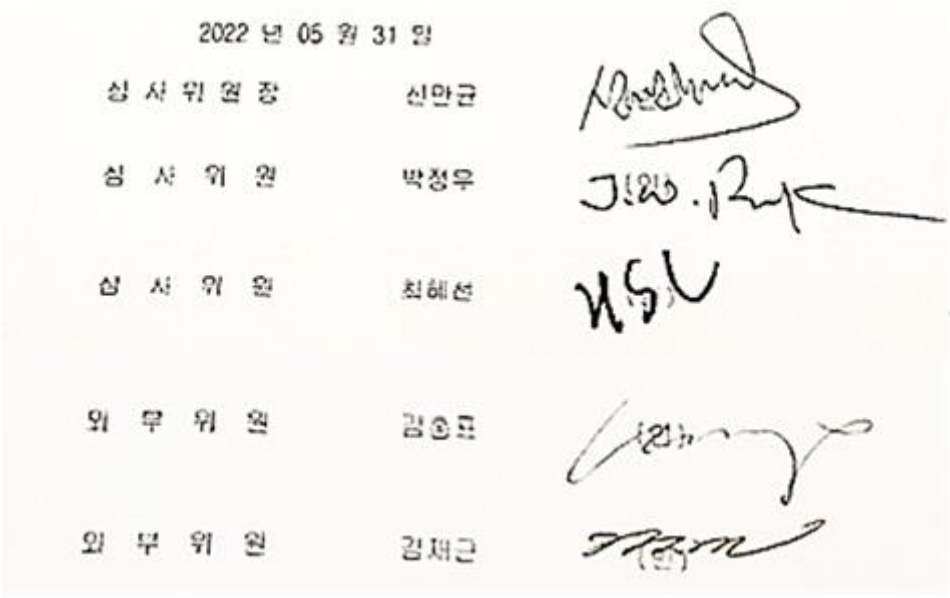

Department of Biological Sciences

Ulsan, Korea

August 2022

Table of contents

List of original publications

The present thesis is based on the following original articles:

1. *Antioxidants* **2020**, *9*(7), 588; doi:10.3390/antiox9070588

Dauricine Protects from LPS-Induced Bone Loss via the ROS/PP2A/NF-κB Axis in Osteoclasts

Hyun-Jung Park , Malihatosadat Gholam Zadeh, Jae-Hee Suh and Hye-Seon Choi

2. *Antioxidants* **2021**, 10, 619. https://doi.org/10.3390/antiox10040619

Estrogen Decreases Cytoskeletal Organization by Forming an ERα/SHP2/c-Src Complex in Osteoclasts to Protect against Ovariectomy-Induced Bone Loss in Mice

Hyun-Jung Park, Malihatosadat Gholam-Zadeh, Sun-Young Yoon , Jae-Hee Suh and Hye-Seon Choi

Abstract

The Bone is a metabolically active organ that undergoes continuous remodeling to have a balanced homeostasis under physiological condition. Tipped balance induces impaired bone metabolism. Excessive bone resorption results in bone loss. We set two animal models for bone loss induced by inflammation and estrogen deficiency.

Lipopolysaccharides (LPS) had been injected in mice to induce inflammatory bone loss. Dauricine (DAC), an isoquinoline alkaloid protected from LPS- induced bone loss. DAC reduced the differentiation and activity of osteoclasts by decreasing ROS via the ROS/PP2A/NF-Kb axis. These results implied the therapeutic potential of DAC against inflammatory bone loss.

In ovariectomy (OVX)- induced bone loss, Estrogen (E2) decreased the bone loss. E2 decreased the size of osteoclasts via blocking a signal for actin ring formation without affecting differentiation. E2 binding to estrogen receptor (ERα) forms a complex with SHP2/c-Src to decrease c-Src activation that was induced upon RANKL stimulation in a non-genomic manner, leading to impaired cytoskeletal organization of osteoclasts and reducing bone resorption.

Chapter 1

Dauricine Protects against Inflammatory bone loss induced by LPS via attenuating ROS/PP2A/NF-κB Axis in Osteoclasts.

1. Introduction

Continuous process of synthesis and resorption of bone for its mature structure and maintenance of calcium level named bone remodeling [1]. While the osteoclasts, giant multinuclear cells, are responsible for bone resorption at diffrent sites, osteoblasts make new bone to maintain the skeletal structure [2,3]. osteoporosis develops slowly over an imbalance between bone formation and bone resorption due to certain pathological conditions including inflammation and estrogen deficiency which can lead to abnormal bone remodeling and the development of bone disorders.

Drastic bone loss can be caused in inflammatory diseases including rheumatoid arthritis, psoriatic arthritis, and Crohn's disease leading increased risk of fracture. Osteoclasts, giant multinuclear cells responsible for bone resorption, will be affected by immune cells and their produced sytokines leading to more bone resorption activity [4,5].

In addition, receptor activator of nuclear factor kappa-B ligand (RANKL), tumor necrosis factor-α (TNF-α), and IL-17 produced by immune cells will contribute to bone loss via affecting osteoclastogenesis [6,7].

In in vivo, lipopolysaccharide (LPS) can induce systemic inflammation leading to bone loss via the activity of OCs [8–10], followed by differentiation, survival, and function of osteoclasts in vitro [11–14].

Hematopoietic cells are differentiated to osteoclast precursors and further matured to osteoclasts active for bone resorption in presence of macrophage colony stimulating factor (M-csf) and Receptor activator of nuclear factor kappa-B ligand (RANKL).

The importance of nuclear factor-kappa B (NF-κB) signaling induced by receptor activator of NF-κB ligand (RANKL) in osteoclastogenesis has been confirmed in our previous studies. RANKL induces the signaling by recruitment of TNF receptor (TNFR)-associated factor 6 (TRAF6), activating a complex consisting of IκB kinase (IKK)-α, IKK-β and IKK-γ (NF-κB essential modulator, NEMO), which induces phosphorylation and degradation of IκB-α leading to release of p65/p50 heterodimers,

which translocate to the nucleus. This induces the expression of two other transcription factors including c-Fos and nuclear factor of activated T-cells, cytoplasmic 1 (NFATc1) which are necessary for osteoclast differentiation. Conditional IKKβ deficiency leads to osteopetrosis with a reduced number of OCs, whereas IKKα is not necessary for osteoclastogenesis in vivo, suggesting a critical role of IKKβ as a signal transducer for NF-κB dimers in OC differentiation [17].

Dauricine (DAC) a natural compound from Rhizoma menispermi, has been reported to be used as traditional Chinese medicine in case of several inflammatory diseases [18–21]. As example, Dauricine ameliorated LPS- induced Acute lung injury (ALI) and inflammation in macrophages via inhibition of nuclear localization and activity of nuclear factor-kappaB (NF-κB) by suppressing the phosphorylation of NF-κB inhibitors (IκB). DAC also decreased the release of pro-inflammatory cytokines including nitric oxide (NO), interleukin-1β (IL1β), IL6, tumor necrosis factor-α (TNFα), inducible nitric oxide synthase (iNOS), and cyclooxygenase-2 (Dauricine induced apoptosis via suppression of nuclear factor-kappaB (NF-kappaB) activation. DAC decreased the phosphorylation and degradation of IkBα and subsequent translocation of p65 in a dose- and time-dependent manner. Eventually, DAC downregulated the expression of NF-kB-target genes including genes related to cell proliferation (cyclinD1, COX2, and c-Myc), anti-apoptosis (survivin, Bcl-2, XIAP, and IAP1), invasion (MMP-9 and ICAM-1), and angiogenesis (VEGF). However, Dauricine also had been found to have neuroprotective effects against Alzheimer's disease (AD), through activation of Nrf2-keap1 pathway and suppression of caspase 3 activity to decrease oxidative stress and apoptosis, respectively. Dauricine has been confirmed as an anti-oxidative and anti-apoptosis agent in therapeutic strategies.

According to others and our publications[9], blocking NF-κB signaling can have a protective effect against bone loss due to inflammation. We hypothesize that dauricin may protect against bone loss due to inflammation by inhibiting NF-κB signaling. In this paper we found that DAC can inhibit

inflammatory bone loss in the LPS-induced animal model and we also investigated the details about the molecular mechanism of DAC in osteoclastogenesis.

2. Material and methods

2.1. OC Formation

Osteoclasts are differentiated from bone marrow cells. Briefly, bone marrow cells are harvested from 4–5-week-old C57BL/6J mice and cultured for 16 hr with α-MEM containing FBS and M-CSF (20 ng/ml). Floating cells were collected and cultured in same condition for more 2 days. Next, bone marrow macrophage/ monocyte lineage cells harvested and differentiated to osteoclasts in presence of M-CSF (30 ng/ml) and RANKL (40 ng/ml) for 55 hours. Then, the pre-OCs were treated with M-CSF (30 ng/ml) and LPS (50 ng/ml) to form Ocs in presence or absence of Dauricine (DAC). After fixation and staining, the number of tartrate-resistant acid phosphatase (TRAP)-positive multinucleated cells (MNCs), area and fusion index as the average number of nuclei per TRAP-positive MNCs were evaluated using imageJ analysis software.

2.2. Cell Viability

To evaluate the cell viability, After differentiation, the cells were washed and incubated for 3 hr with MTT (3-(4,5-dimethylthiazol-2-yl)-2,5-diphenyltetrazolium bromide) at 37℃. After removal of MTT, reduced MTT crystals (formazan) dissolved in DMSO (Dimethyl sulfoxide), resulting in colored solution. The absorbance was measured at 540 nm with a microplate reader.

2.3. RNA Isolation and Quantitative Polymerase Chain Reaction (qPCR)

Total RNA was isolated by QIAzol lysis reagent and reverse- transcribed to cDNA with M-MLV reverse transcriptase and random primers. Next, qPCR was performed using SYBR Green Real-Time PCR Mater Mixes and related primers in MicroAmp Fast Reaction Tubes (8 tubes/strip) (Applied Biosystems, Foster City, CA, USA) using the StepOnePlus™ Real Time System (Applied Biosystems). The formula 2-ΔΔCt was used for calculation the Relative gene expression and the housekeeping gene 18S rRNA (RPS) used for normalization.

Gene name	Forward sequence 5´- 3´	Reverse sequence 5´- 3´
ATP6v0d2	AGCAAAGAAGACAGGGAG	CAGCGTCAAACAAAGG
Cathepsin K	GGGCCAGGATGAAAGTTGTA	CACTGCTCTCTTCAGGGCTT
Calcitonin receptor	AGTTGCCCTCTTATGAAGGAGAAG	GGAGTGTCGTCCCAGCACAT
DC-STAMP	TCCTCCATGAACAAACAGTTCCAA	AGACGTGGTTTAGGAATGCAGCTC
TRAP	GACCACCTTGGCAATGTCTCTG	TGGCTGAGGAAGTCATCTGAGTTG
RPS	ATCAGAGAGTTGACCGCAGTTG	AATGAACCGAAGCACACCATAG

2.4. Bone Resorption

To evaluate the bone resorption activity of OCs, mature osteoclasts are incubated on dentine slices for 3- 5 days. In summary, Pre-osteoclasts were cultured with M-CSF and RANKL to obtain mature Ocs, then harvested and seeded on top of the dentine slices for further incubation with M-CSF (30 ng/mL) and LPS (50 ng/mL) in the presence or absence of DAC (7 μM) for 4 days. The cells were stained for TRAP, then removed by ultrasonication in 1M NH4OH and stained with 1% (w/v) toluidine blue in 0.5% sodium borate to visualize resorption pits. ImageJ software, 1.37v was used for measuring Resorption pit area.

2.5. Western Blot Analysis

Total Protein extraction is done using lysis buffer (50 mM Tris-HCl, pH 8.0, 150 mM NaCl, 1 mM EDTA, 0.5% Nonidet P-40, and 0.01% protease inhibitor mixture) and Nuclear/Cytosol Fractionation Kit. Proteins were separated by SDS-PAGE and transferred to nitrocellulose membranes. After blocking with 5% skim milk in Tris-buffered saline which contained 0.1% Tween 20% (1x TBS-T) for 1 h at room temperature, the membrane was incubated with primary antibodies against phospho-IKKα/β (S176/180) (#2697, Cell Signaling, Danvers, MA, USA), lamin B (#13435, Cell Signaling), p65 (sc-372, Santa Cruz Biotechnology, Santa Cruz, CA, USA), PP2A (sc-13600, Santa Cruz Biotechnology), and β-actin (A5441, Sigma–Aldrich) overnight at 4° C. Next, the membrane was incubated with secondary antibodies for 1 hour after washing with 1x TBS-T and developed with chemiluminescent substrates.

2.7. Transfection of siRNA

Pre-osteoclasts after 40 hours incubation with M-CSF and RANKL, transfected with small interfering RNA (siRNA) against PP2A or scrambled siRNA (scRNA) using Lipofectamine 3000. Briefly, 2.5 μL of both siRNA and scRNA which were mixed with 3.75 μL of lipofectamine 3000 reagent in 50 μL Opti-MEM separately. After incubation for 15 mins, the mixtures were added to cells and further incubated with M-CSF (30 ng/ml) and LPS (50 ng/ml) in presence or absence of DAC (7 μM).

2.8. Statistical Analysis

All experiments were repeated at least three times. The data are expressed as the mean ± standard deviation and a p value less than 0.05 was considered statistically significant. Statistical analysis was performed using Student's t-test when two groups were compared or by one-way ANOVA followed by Bonferroni posttests when multiple groups were compared. Two-way ANOVA was used when two variables were analyzed.

3. Results

3.1. LPS induced osteoclastogenesis is inhibited by DAC in vitro

It has been shown that protection effect of DAC in murine model of LPS induced bone loss is through osteoclast since the number of TRAP positive osteoclast is decreased significantly. To investigate whether DAC can decrease differentiation and activity of osteoclast in vitro, the pre-osteoclasts treated with LPS with or without DAC. After 48h, DAC decreased number and area of TRAP positive multinuclear cells (MNCs) significantly upon LPS stimulation (Figure 1A). To check the toxicity of DAC on osteoclast, MTT assay was performed and cells were not affected by DAC (Figure 1B). The mRNA expression level of specific genes involved in differentiation of osteoclasts including TRAP, calcitonin receptor, cathepsin K, DC-STAMP, and ATP6v0d2 is increased in presence of LPS while, it is reduced dramatically under treatment with DAC (Figure 1C). Next, we assessed the effect of DAC on bone resorption activity of osteoclast in vitro via using dentine slices. Pre- osteoclast differentiated to mature osteoclast and seeded on dentine slices. The cells further incubated with LPS in presence or absence of DAC. As shown in Figure 1D, DAC attenuated bone resorption activity counted by total pit area/ number of Ocs. Together, these results show that DAC can decrease the differentiation and bone resorption activity of osteoclasts.

3.2. DAC Decreases Up- Regulation of Cytosolic Reactive Oxygen Species (cROS) and subsequent NF-KB pathway activated by LPS in pre- osteoclasts

Since the previous study in our lab showed bone loss induced by LPS can be pretected via blockage of NF-kB activity in osteoclast [9] and DAC has been reported as anti-inflammatory drug and inhibitor of NF-κB activaty [19, 20], we assumed that DAC may inhibit the differentiation and activity of osteoclast via NF-kB signaling in LPS- induced osteoclastogenesis.

To assess this hypothesis, we considered pharmacological inhibitors of NF-KB signaling pathway: JSH23, the blocker of nuclear translocation of p65 and BAY 11-7082, inhibitor of IκBα phosphorylation. The pre-osteoclasts were treated with LPS and DAC in presence or absence of above mentioned inhibitors. Number and area of TRAP positive MNCs were reduced in presence of both inhibitors upon stimulation with LPS while in co- treatment of DAC along with JSH23 and BAY 11-7082, any significant effect of DAC was not observed on LPS- induced osteoclastogenesis (Figure 2A).

It has been already shown that LPS can induce osteoclastogenesis via increasing both ROS level of cytosol [12] and mitochondrial (mROS) [10]. That made us wondering whether DAC can attenuate ROS level to prevent LPS effect on osteoclastogenesis. No changes were observed in mitocondrial ROS in response to DAC while the cytosol ROS stimulated by LPS decreased significantly in presence of DAC (Figure 2B). Next we assessed the role of ROS in blockage effect of DAC in LPS-induced Ocs, via N-acetyl cysteine (NAC), a scavenger of ROS and diphenyleneiodonium chloride (DPI), an inhibitor of NADPH oxidase. As shown in Figure 2C, in co- treatment of DAC with NAC and DPI, the effect of DAC on reducing number and area of osteoclasts was totally abolished while both NAC and DPI decreased dramatically the number and area of osteoclasts upon stimulation with LPS.

3.3. DAC Decreases Oxidation of PP2A by ROS to Block NF-kB Activation upon LPS stimulation

Based on previous results, both inhibited NF-kB signaling and reduced cytosolic ROS were involved in prevention of LPS-induced osteoclastogenesis by DAC. We considered both pathways were related to molecular mechanism of DAC. So we assumed effect of DAC in decreasing ROS level may modify the target molecules implicated in inhibition of NF-kB signaling.

Kray and colleagues showed inactivation of serine/threonine-protein phosphatase 2A (PP2A) leads to activation of IKKα/IκBα/NF-κB signaling pathway [26]. It has been reported that ROS can mediate

inactivation of PP2A promoting NF-kB pathway [27]. So we hypothesized that mechanism of DAC in decreasing LPS- induced osteoclastogenesis is related to blockage of ROS oxidizing PP2A leading to NF-κB activation.

To check whether DAC reduced the oxidized form of PP2A to attenuate NF-κB signaling, the protein level of reduced PP2A and phosphorylated IKKα/β was assessed upon LPS stimulation with or without DAC. Effect of LPS on alleviating the reduced form of PP2A and subsequent increase of phosphorylated IKKα/β regained with DAC as shown in Figure 3A. Further, the nuclear localization of p65 which was increased upon exposure of LPS was attenuated significantly by DAC (Figure 3A). Next, we silenced PP2A by using small interfering RNA to confirm the role of PP2A in molecular mechanism of DAC. The inhibitory effect of DAC on number, area and fusion index of osteoclasts was completely disrupted in cells silenced for PP2A while scRNA treated cells did not show any significant change in presence or absence of DAC upon LPS stimulation (Figure 3B).

3.4. DAC Decreases Differentiation and Activity of OCs upon RANKL Stimulation In Vitro

Receptor activator of nuclear factor kappa-B ligand (RANKL) is required for differentiation of osteoclasts. Upon binding of RANKL to RANK, the receptor on surface of osteoclasts, the recruitment of TRAF6 (TNF Receptor Associated Factor 6) will lead to activation of NF-kB signaling pathway and osteoclastogenesis. Based on previous data, DAC has the ability to inhibit the NF-kB pathway which is induced by LPS in osteoclasts. To confirm the role of DAC in prevention of RANKL/NF-kB signaling pathway, the bone marrow macrophage/ monocyte lineage cells treated with RANKL in presence or absence of DAC. Osteoclastogenesis is attenuated significantly by DAC in dose dependent manner (Figure 4A). The expression level of genes specific for osteoclasts was also decreased significantly upon exposure of DAC (Figure 4B).

4.Disscussion

It has been demonstrated that DAC, an isoquinoline alkaloid has anti-inflammatory activity [18,19]. LPS decreased dramatically the bone mass while the mices injected with DAC showed higher bone density implyed that DAC has protective effect against inflammatory bone loss.

Based on in vivo expriments, the inflammation induced by LPS can cause bone loss due to increased number of osteoclasts while the serum level of Alkaline phosphatase (ALP) and osteocalcin did not show any significant alteration, suggesting the bone loss stimulated with LPS is related to higher number and activity of osteoclasts. Bone remodeling can be affected in some pathological conditions and bone resorption will be un-coupled from bone formation. For example in case of bone loss induced by ovariectomy [24, 28] and cholesterol [29] coupled bone remodeling was observed while in LPS- induced bone loss model , bone remodeling was uncoupled due to in vivo results. Uncoupled bone remodeling has been mentioned previously in some bone diseases including Multiple myeloma, a type of bone marrow cancer[30] and osteoporosis related to progranulin [31]. Inflammation is involved in periodontal bone loss via limitation of bone formation [32].

The level of MCP-1 and ROS in supernatant of cells treated with LPS increased significantly while in presence of DAC the level of ROS and MCP-1 decreased significantly, suggesting that DAC reduced the oxidative stress and subsequent inflammation in cells treated with LPS. These results have been confirmed in animal model of LPS- induced bone loss with or without DAC.

DAC not only decreased osteoclast differentiation but also the activity of osteoclast attenuated significantly on dentine slices in vitro. The expression level of genes related to osteoclastogenesis in cells treated with DAC down- regulated remarkably compared with cells under exposure of LPS only.

Comapring to control, DAC alone didnt show any difference in bone mass while in vitro, decreased both RANKL- induced osteoclastogenesis and genes specific to osteoclasts dramatically . The reason could be related to lower level of RANKL under physiological condition compare with in vitro conditions. The up- regulation of RANKL can be observed in some pathological conditions including loss of ovarian function [33].

In addition to invivo results, maximum protection is observed upon dose of 2.5 mg/kg of DAC. The higher volume of Bone in DAC treated group comparing to LPS injected group, is related to decreased number of osteoclast, while in femure sections of bone after staining no significant change is observed in number of osteoblast compared with LPS treated group. The effect of DAC in protecting LPS induced bone loss is not observed at higher dose due to less bone formation.

It has been indicated that DAC is efficiently protective against ischemia/reperfusion induced inflammation at dose of 5-10 mg/kg [18] in rodents. 5–20 mg/kg and 6–12 mg/kg of DAC was sufficient to prevent lung injury induced by cecal ligation and puncture and pancreatic tumor growth [19, 34].

The potential effect of DAC to suppress the activity of NF-kB pathway is observed in macrophages in dose of 1-10 μM and in colon cancer cells within the range of 5–40 μM [19, 20].

It has been reported that the plasma level of DAC reached to 16 μg/mL after 15 min of 15 mg/kg intravenous injection of DAC [35]. Following the same pattern to apply, injection dose of 2.5 mg/kg could derive a serum level of 2.7 μg/mL which is in the range of our invitro used concentration of DAC.

Healthy males in the study performed by Liu and colleagues [36] received DAC in range of 60-180 mg voluntearily, so it is reasonable that 2.5 mg/kg dose (equivalent to 150 mg/60 kg) can be used for translational experiments in vivo.

To investigate the molecular mechanism of DAC on osteoclasts stimulated with LPS, the pre-osteoclasts treated with LPS with or without DAC. LPS can affect the differentiation of osteoclast positively via activation of NF-kB signaling pathway [9]. The pre-osteoclasts treated with LPS next to pharmacological inhibitors of NF-kB sinaling: BAY 11-7082, inhibitor of IκBα phosphorylation and JSH23, inhibitor of nuclear translocation of the p65 subunit of NF-kB in presence or absence of DAC. Both inhibitors and DAC decreased the number and area of osteoclasts significantly while in co- treatment, the effect of DAC was abolished on osteoclastogenesis stimulated by LPS, implying that main effect of DAC is related to inhibition of NF-kB signaling. On the other side, the up-regulated ROS by LPS decreased dramatically under treatment with DAC.

To check the effect of DAC on LPS- induced ROS, the pre- osteoclasts treated with LPS and N-acetyl-L-cysteine (NAC), a ROS scavenger and Diphenyleneiodonium chloride (DPI), inhibitor of NADPH oxidase, in presence or absence of DAC. Co- treatment of inhibitors and DAC attenuated the effect of DAC on number and area of osteoclasts, demonstrating that reduced level of ROS is involved in molecular mechanism of DAC in prevention of LPS- induced osteoclastogenesis.

PP2A, Protein phosphatase 2, is known as negative regulator of NF-kB signaling pathway and inactivation of PP2A will lead to phosphorylation of IKKα/β and nuclear localization of NF-kB subunits p65 and p50 to activate the transcription of genes. Oxidation of PP2A by ROS upon LPS exposure is responsible for activation of NF-kB signaling in pre- osteoclast while DAC will decrease the ROS level leading to reduction form of PP2A and inactivation of NF-kB signaling.

NADPH oxidase inhibitor, DPI, decreased the oxidized form of PP2A, indicating that ROS is acting as up-stream modulator of PP2A and subsequent NF-kB signaling pathway.

Silencing of PP2A by small interfering RNA (siRNA) will disrupt the the effect of DAC in decreasing number and area of osteoclasts, demonstating that PP2A is involved in prevention effect of DAC in LPS- induced osteoclastogenesis via ROS/PP2A/NF-kB pathway.

In previous studies the importance of ROS in activation of NF-kB signaling have been also proven [27, 37, 38] but the details about molecular mechanism of ROS in modulation of NF-kB signaling is not completely known. The mechanism of ROS might be specific in different type of cell [37] but upon direct exposure of ROS in Jurkat T cells, the NF-kB signaling is activated significantly [39].

In endothelial cells of human, inactivation of PP2A and SHP2 as negative regulators, by ROS is involved in activation of NF-kB signaling [40]. Our results together showed that increased ROS level is responsible for oxidation of PP2A leading to suppression of enzymatic activity of PP2A and subsequent phosphorylation of IKKα/β and localization of p65 to nucleus. So the inhibitory effect of DAC is related to suppression of ROS/PP2A/IKKα/β/p65 through reducing the cytosolic level of ROS [41,42].

5. Conclusions

In summary, these results concluded that DAC can protect against inflammatory induced bone loss via decreasing ROS level and activating PP2A. Subsequent reduction of PP2A will lead to suppression of NF-kB signaling pathway in osteoclasts, proposing that PP2A can be considered as potential target in treatment of bone loss stimulated by inflammation.

References

1. Van Staa, T.P.; Geusens, P.; Bijlsma, J.W.; Leufkens, H.G.; Cooper, C. Clinical assessment of the long-term risk of fracture in patients with rheumatoid arthritis. Arthritis Rheum. 2006, 54, 3104–3112.

2. Kocijan, R.; Englbrecht, M.; Haschka, J.; Simon, D.; Kleyer, A.; Finzel, S.; Kraus, S.; Resch, H.; Muschitz, C.; Engelke, K.; et al. Quantitative and Qualitative Changes of Bone in Psoriasis and Psoriatic Arthritis Patients. J. Bone. Miner. Res. 2015, 30, 1775–1783.

3. Haschka, J.; Hirschmann, S.; Kleyer, A.; Englbrecht, M.; Faustini, F.; Simon, D.; Figueiredo, C.P.; Schuster, L.; Muschitz, C.; Kocijan, R.; et al. High-resolution Quantitative Computed Tomography Demonstrates Structural Defects in Cortical and Trabecular Bone in IBD Patients. J. Crohns. Colitis. 2016, 10, 532–540.

4. Pasco, J.A.; Kotowicz, M.A.; Henry, M.J.; Nicholson, G.C.; Spilsbury, H.J.; Box, J.D.; Schneider, H.G. High-Sensitivity C-Reactive Protein and Fracture Risk in Elderly Women. JAMA 2006, 296, 1353–1355.

5. Gravallese, E.M.; Harada, Y.; Wang, J.T.; Gorn, A.H.; Thornhill, T.S.; Goldring, S.R. Identification of Cell Types Responsible for Bone Resorption in Rheumatoid Arthritis and Juvenile Rheumatoid Arthritis. Am. J. Pathol. 1998, 152, 943–951.

6. Dewhirst, F.E.; Stashenko, P.P.; Mole, J.E.; Tsurumachi, T. Purification and Partial Sequence of Human Osteoclast-Activating Factor: Identity with Interleukin 1 Beta. J. Immunol. 1985, 135, 2562–2568.

7. Redlich, K.; Smolen, J.S. Inflammatory Bone Loss: Pathogenesis and Therapeutic Intervention. Nat. Rev Drug Discov. 2012, 11, 234–250.

8. Orcel, P.; Feuga, M.; Bielakoff, J.; De Vernejoul, M.C. Local Bone Injections of LPS and M-CSF Increase Bone Resorption by Different Pathways In Vivo in Rats. Am. J. Physiol. 1993, 264, E391–E397.

9. Park, H.J.; Son, H.J.; Sul, O.J.; Suh, J.H.; Choi, H.S. 4-Phenylbutyric Acid Protects Against Lipopolysaccharide-Induced Bone Loss by Modulating Autophagy in Osteoclasts. Biochemical. Pharmacol. 2018, 151, 9–17.

10. Park, H.J.; Gholam-Zadeh, M.; Suh, J.H.; Choi, H.S. Lycorine Attenuates Autophagy in Osteoclasts via an Axis of Mros/TRPML1/TFEB to Reduce LPS-Induced Bone Loss. Oxid. Med. Cell. Longev. 2019, 8982147.

11. Park, H.; Noh, A.L.; Kang, J.H.; Sim, J.S.; Lee, D.S.; Yim, M. Peroxiredoxin II Negatively Regulates Lipopolysaccharide-Induced Osteoclast Formation and Bone Loss via JNK and STAT3. Antioxid. Redox Signal. 2015, 22, 63–77.

12. Sul, O.J.; Park, H.J.; Son, H.J.; Choi, H.S. Lipopolysaccharide (LPS)-Induced Autophagy Is Responsible for Enhanced Osteoclastogenesis. Mol. Cells. 2017, 40, 880–887.

13. Sul, O.J.; Rajasekaran, M.; Park, H.J.; Suh, J.H.; Choi, H.S. MicroRNA-29b Enhances Osteoclast Survival by Targeting Bcl2-Modifying Factor after Lipopolysaccharide Stimulation. Oxid. Med. Cell. Longev. 2019, 6018180.

14. Sul, O.J.; Sung Y., B.; Rajasekaran, M.; Ke, K.; Yu, R.; Back, S.H.; Choi, H.S. MicroRNA-155 Induces Autophagy in Osteoclasts by Targeting Transforming Growth Factor B-Activated Kinase 1-Binding Protein 2 upon Lipopolysaccharide Stimulation. Bone 2018, 116, 279–289.

15. Iotsova, V.; Caamaño, J.; Loy, J.; Yang, Y.; Lewin, A.; Bravo, R. Osteopetrosis in Mice Lacking NF-kappaB1 and NF-kappaB2. Nat. Med. 1997, 3, 1285–1289.

16. Jimi, E.; Takakura, N.; Hiura, F.; Nakamura, I.; Hirata-Tsuchiya, S. The Role of NF-κB in Physiological Bone Development and Inflammatory Bone Diseases: Is NF-κB Inhibition “Killing Two Birds with One Stone? Cells. 2019, 8, 1636.

17. Ruocco, M.G.; Maeda, S.; Park, J.M.; Lawrence, T.; Hsu, L.C.; Cao, Y.; Schett, G.; Wagner, E.F.; Karin, M. I{kappa}B Kinase (IKK){beta}, but not Ikk{Alpha}, is a Critical Mediator of Osteoclast Survival and is Required for Inflammation-Induced Bone Loss. J. Exp. Med. 2005, 201, 1677–1687.

18. Yang, X.Y.; Jiang, S.Q.; Zhang, L.; Liu, Q.N.; Gong, P.L. Inhibitory Effect of Dauricine on Inflammatory Process Following Focal Cerebral Ischemia/Reperfusion in Rats. J. Chin. Med. 2007, 35, 477–486. [CrossRef] [PubMed] Antioxidants 2020, 9, 588 14 of 15

19. Qiao, B.; Wang, H.; Wang, C.; Liang, M.; Huang, K.; Li, Y. Dauricine Negatively Regulates Lipopolysaccharide- or Cecal Ligation and Puncture-Induced Inflammatory Response via NF-κB inactivation. Arch. Biochem. Biophys. 2019, 666, 99–106.

20. Yang, Z.; Li, C.; Wang, X.; Zhai, C.; Yi, Z.; Wang, L.; Liu, B.; Du, B.; Wu, H.; Guo, X.; et al. Dauricine Induces Apoptosis, Inhibits Proliferation and Invasion Through Inhibiting NF-kappaB Signaling Pathway in Colon Cancer Cells. J. Cell. Physiol. 2010, 225, 266–275.

21. Wang, L.; Pu, Z.; Li, M.; Wang, K.; Deng, L.; Chen, W. Antioxidative and Antiapoptosis: Neuroprotective Effects of Dauricine in Alzheimer’s Disease Models. Life Sci. 2020, 243, 117237.

22. Zhao, X.; Shen, J.; Chang, K.J.; Kim, S.H. Comparative Analysis of Antioxidant Activity and Functional Components of the Ethanol Extract of Lotus (Nelumbo Nucifera) from Various Growing Regions. J. Agric. Food. Chem. 2014, 62, 6227–6235.

23. Gao, Y.; Grassi, F.; Ryan, M.R.; Terauchi, M.; Page, K.; Yang, X.; Weitzmann, M.N.; Pacifici, R. Ifn-Gamma Stimulates Osteoclast Formation and Bone Loss In Vivo via Antigen-Driven T Cell Activation. J. Clin. Investig. 2007, 117, 122–132.

24. Van Phan, T.; Sul, O.J.; Ke, K.; Lee, M.H.; Kim, W.K.; Cho, Y.S.; Kim, H.-J.; Kim, S.-Y.; Chung, H.-T.; Choi, H.S. Carbon Monoxide Protects against Ovariectomy-Induced Bone Loss by Inhibiting Osteoclastogenesis. Biochem. Pharmacol. 2013, 85, 1145–1152.

25. Jimi, E.; Akiyama, S.; Tsurukai, T.; Okahashi, N.; Kobayashi, K.; Udagawa, N.; Nishihara, T.; Takahashi, N.; Sudaet, T. Osteoclast Differentiation Factor Acts as a Multifunctional Regulator in Murine Osteoclast Differentiation and Function. J. Immunol. 1999, 163, 434–442.

26. Kray, A.E.; Carter, R.S.; Pennington, K.N.; Gomez, R.J.; Sanders, L.E.; Llanes, J.M.; Khan, W.N.; Ballard, D.W.; Wadzinski, B.E. Positive Regulation of Ikappab Kinase Signaling by Protein Serine/Threonine Phosphatase 2a. J. Biol. Chem. 2005, 280, 35974–35982.

27. Chattopadhyay, R.; Mani, A.M.; Singh, N.K.; Rao, G.N. Resolvin D1 Blocks H2o2 -Mediated Inhibitory Crosstalk Between Shp2 and Pp2a and Suppresses Endothelial-Monocyte Interactions. Free. Radic. Biol. Med. 2018, 117, 119–131.

28. Jilka, R.L.; Takahashi, K.; Munshi, M.; Williams, D.C.; Roberson, P.K.; Manolagas, S.C. Loss of Estrogenupregulates Osteoblastogenesis in the Murine Bone Marrow. Evidence for Autonomy from Factors Released During Bone Resorption. J. Clin. Invest. 1988, 101, 1942–1950.

29. Sul, O.J.; Kim, J.E.; Ke, K.; Suh, J.H.; Choi, H.S. Atherogenic Diet-Induced Bone Loss is Primarily Due to Increased Osteoclastogenesis in Mice. J. Nutr. Biochem. 2002, 79, 108337.

30. Terpos, E.; Ntanasis-Stathopoulos, I.; Gavriatopoulou, M.; Dimopoulos, M.A. Pathogenesis of Bone Disease in Multiple Myeloma: From Bench to Bedside. Blood Cancer J. 2018, 8, 7.

31. Wang, L.; Roth, T.; Nakamura, M.C.; Nissenson, R.A. Female-Specific Role of Progranulin to Suppress Bone Formation. Endocrinology 2019, 160, 2024–2037.

32. Graves, D.T.; Li, J.; Cochran, D.L. Inflammation and Uncoupling as Mechanisms of Periodontal Bone Loss. J. Dent. Res. 2011, 90, 143–153.

33. Kósa, K.P.; Balla, B.; Kiss, J.; Podani, J.; Takács, I.; Lazáry, A.; Nagy, Z.; Bácsi, K.; Karsai, A.; Speer, G.; et al. Postmenopausal Expression Changes of Immune System-Related Genes in Human Bone Tissue. J. Clin. Immunol. 2009, 29, 761–768.

34. Zhang, Y.B.; Fei, H.X.; Guo, J.; Zhang, X.J.; Wu, S.L.; Zhong, L.L. Dauricine Suppresses the Growth of Pancreatic Cancer In Vivo by Modulating the Hedgehog Signaling Pathway. Oncol. Lett. 2019, 18, 4403–4414.

35. Dong, P.L.; Han, H.; Zhang, T.Y.; Yang, B.; Wang, Q.H.; Eerdun, G.-W. P-glycoprotein Inhibition Increases the Transport of Dauricine Across the Blood-Brain Barrier. Mol. Med. Rep. 2014, 9, 985–988.

36. Liu, X.; Liu, Q.; Wang, D.; Wang, X.; Zhang, P.; Xu, H.; Zhao, H.; Zhao, H. Validated Liquid Chromatography-Tandem Mass Spectrometry Method for Quantitative Determination of Dauricine in Human Plasma and Its Application to Pharmacokinetic Study. J. Chromatogr. B Analyt. Technol. Biomed. Life Sci. 2010, 878, 1199–1203.

37. Li, N.; Karin, M. Is NF-kappaB the Sensor of Oxidative Stress? FASEB J. 1999, 13, 1137–1143. Antioxidants 2020, 9, 588 15 of 15

38. Schreck, R.; Rieber, P.; Baeuerle, P.A. Reactive Oxygen Intermediates As Apparently Widely Used Messengers in the Activation of the NF-Kappa B Transcription Factor and HIV-1. EMBO J. 1991, 10, 2247–2258.

39. Takada, Y.; Mukhopadhyay, A.; Kundu, G.C.; Mahabeleshwar, G.H.; Singh, S.; Aggarwal, B.B. Hydrogen Peroxide Activates NF-{kappa}B Through Tyrosine Phosphorylation of I{kappa}B{alpha} and Serine Phosphorylation of p65: Evidence for the Involvement of I{kappa}B{alpha} Kinase and Syk Protein-Tyrosine Kinase. J. Biol. Chem. 2003, 278, 24233–24241.

40. Gloire, G.; Charlier, E.; Rahmouni, S.; Volanti, C.; Chariot, A.; Erneux, C.; Piette, J. Restoration of SHIP-1 Activity in Human Leukemic Cells Modifies NF-Kappab Activation Pathway and Cellular Survival upon Oxidative Stress. Oncogene 2006, 25, 5485–5494.

41. Storz, P.; Toker, A. Protein Kinase D Mediates a Stress Induced NF-Kappab Activation and Survival Pathway. EMBO J. 2003, 22, 109–120.

42. Fan, C.; Li, Q.; Ross, D.; Engelhardt, J.F. Tyrosine Phosphorylation of I Kappa B Alpha activates NF Kappa B Through a Redox-Regulated and c-Src-Dependent Mechanism Following Hypoxia /Reoxygenation. J. Biol. Chem. 2003, 278, 2072–2080.

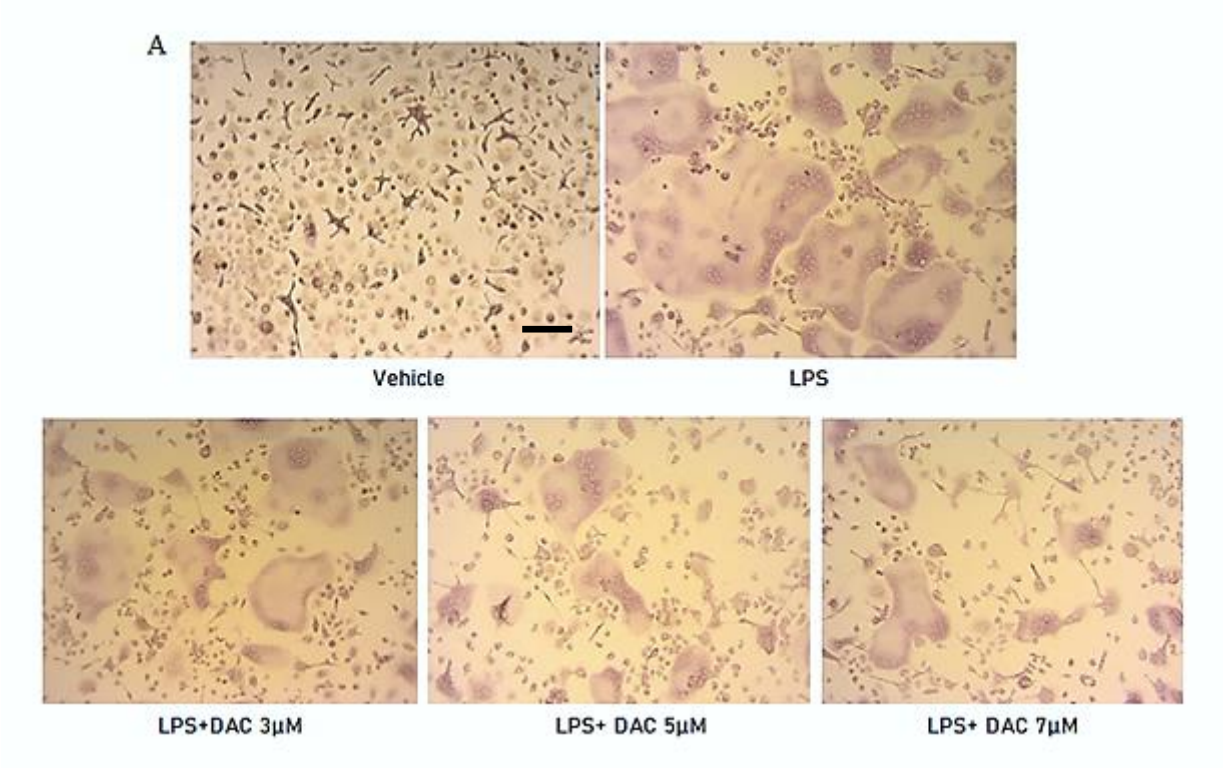
A
Vehicle
LPS
LPS+DAC 3μM
LPS+ DAC 5μM
LPS+ DAC 7μM

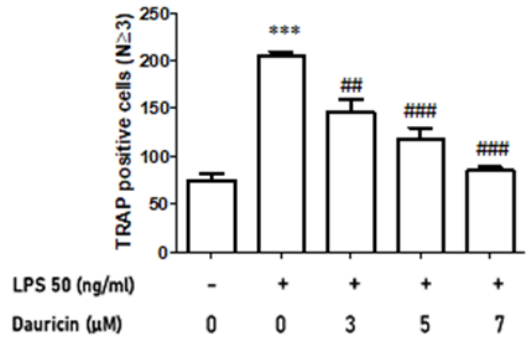
TRAP positive cells (N≥3)
250
200
150
100
50
0
***
##
###
###
LPS 50 (ng/ml) - + + + +
Dauricin (μM) 0 0 3 5 7

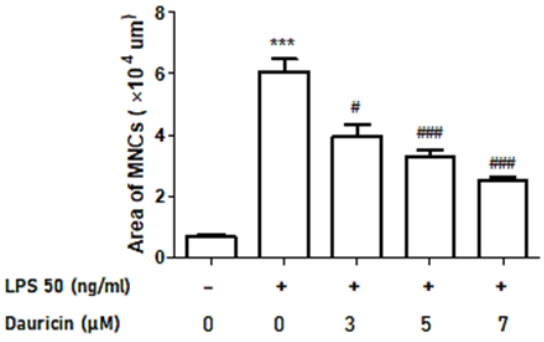
Area of MNCs (×10⁴ um²)
8
6
4
2
0
***
#
###
###
LPS 50 (ng/ml) - + + + +
Dauricin (μM) 0 0 3 5 7

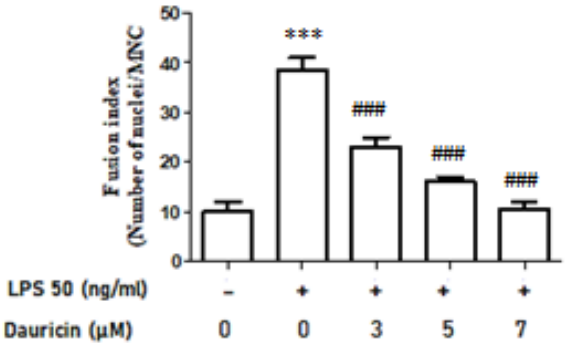
Fusion index
(Number of nuclei/MNC
50
40
30
20
10
0
***
###
###
###
LPS 50 (ng/ml) - + + + +
Dauricin (μM) 0 0 3 5 7

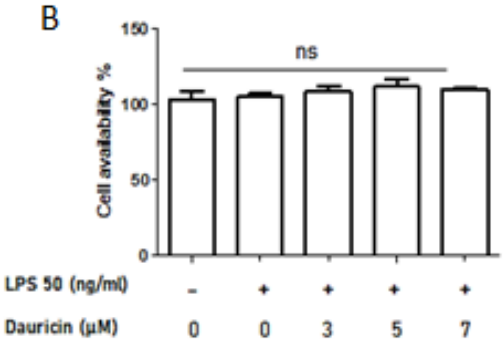
B
Cell availability %
150
100
50
0
ns
LPS 50 (ng/ml) - + + + +
Dauricin (μM) 0 0 3 5 7

C

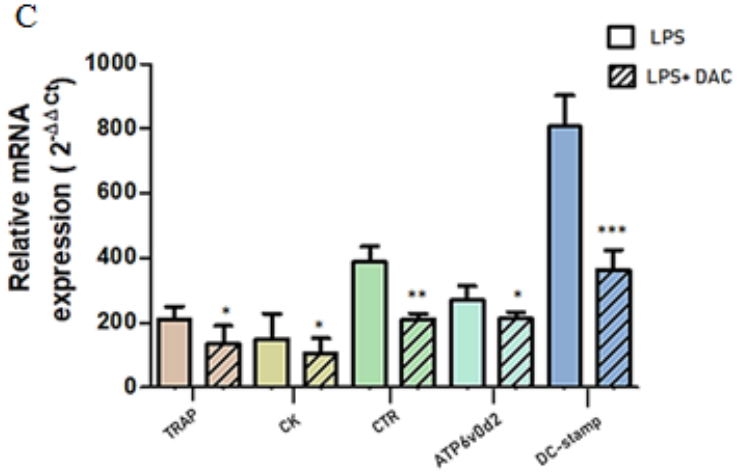
LPS
LPS+ DAC
Relative mRNA expression ($2^{-\Delta\Delta Ct}$)
1000
800
600
400
200
0
*
*
**
*
***
TRAP
CK
CTR
ATP6v0d2
DC-stamp

D

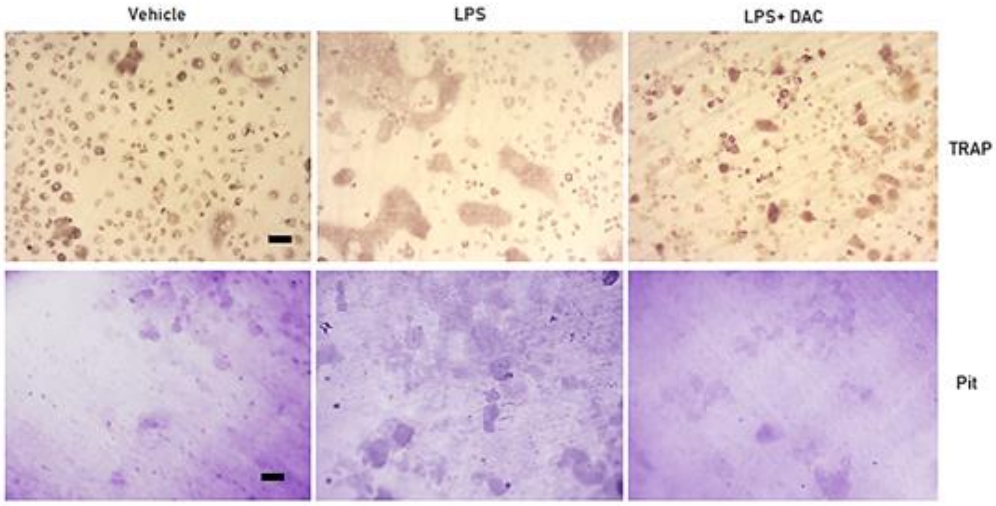
Vehicle
LPS
LPS+ DAC
TRAP
Pit

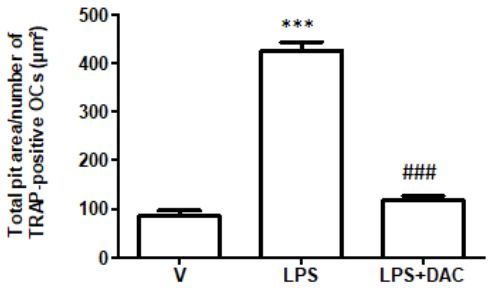
Total pit area/number of TRAP-positive OCs (μm²)
500
400
300
200
100
0
***
###
V
LPS
LPS+DAC

Figure 1. Differentiation and activity of osteoclasts upon LPS stimulation is decreased via DAC in dose dependent manner *in vitro*.

Bone marrow derived macrophages (BMMs) were treated with M-CSF (30 ng/mL) and RANKL (40 ng/mL) for 40 h and pre-osteoclasts further incubated with M-CSF and LPS (50 ng/mL) with or without DAC (3 µM, 5 µM, or 7 µM) (A, B, C). After fixation and TRAP staining, TRAP- positive multinucleated cells (MNCs) were counted. 70≥ cells were selected randomly for measuring the area and fusion index (average of nuclei number/ TRAP positive MNCs). Scale bar: 100µm in the representative OC photos (A). To measure the cell viability, MTT assay was used to compare the cells treated with different concentration of DAC with PBS-treated cells (B). qPCR was performed to check the effect of DAC (7µM) on LPS- induced expression of genes specific to osteoclasts. The expression level is normalized to RANKL pre- treated cells (C). To assess the bone resorption activity of osteoclasts, mature OCs were harvested and incubated more on dentine slices and treated with M-CSF and LPS in presence or absence of DAC (7µM) for 4 days. After TRAP staining, the cells removed by sonification and slices were stained with toluidine blue to make the resorbed area vissible. Photos of TRAP- positive MNCs and resorped pits are represented in scale bar of 100 µm (D). * $p < 0.05$; ** $p < 0.01$; *** $p < 0.001$ compared with PBS-treated pre-OCs. # $p < 0.05$; ## $p < 0.01$; ### $p < 0.001$ compared with LPS-treated cells. Similar results were obtained from three independent experiments.

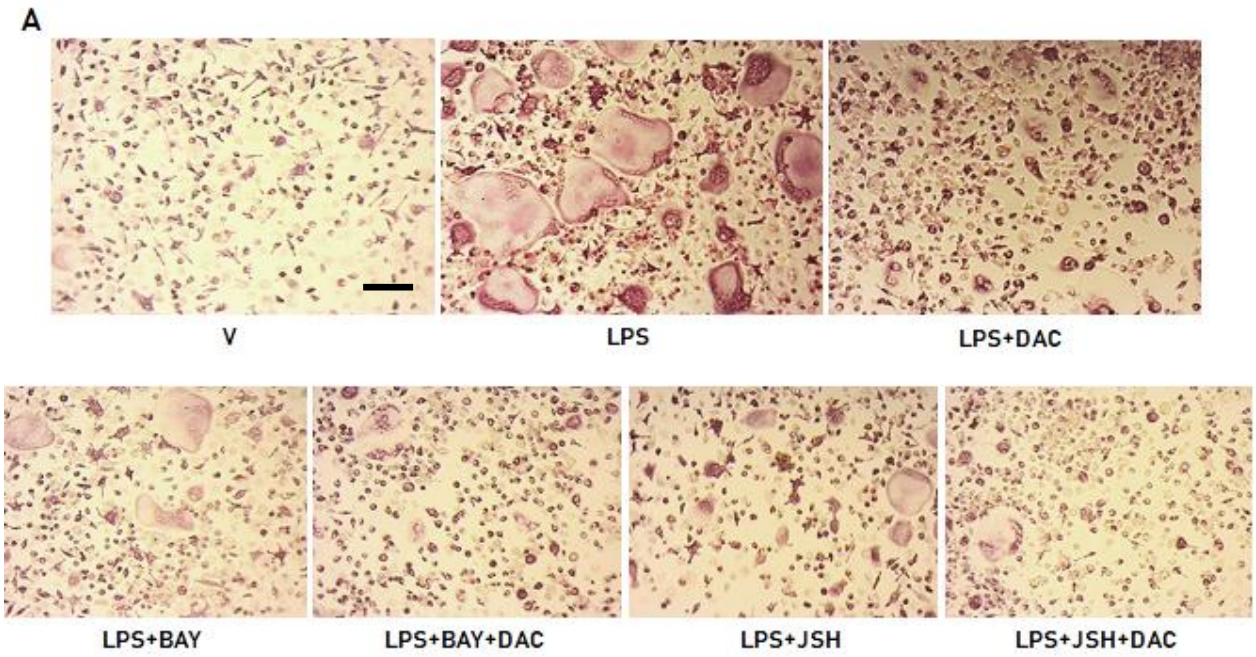
A
V
LPS
LPS+DAC
LPS+BAY
LPS+BAY+DAC
LPS+JSH
LPS+JSH+DAC

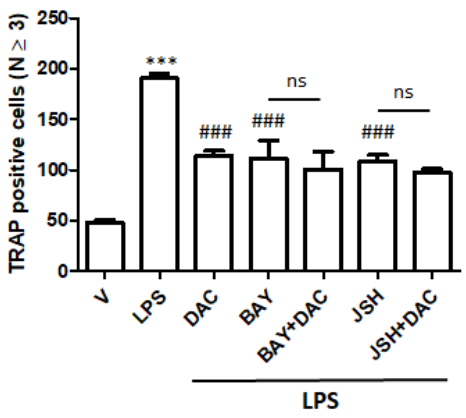
TRAP positive cells (N ≥ 3)
250
200
150
100
50
0
***
###
###
###
ns
ns
V
LPS
DAC
BAY
BAY+DAC
JSH
JSH+DAC
LPS

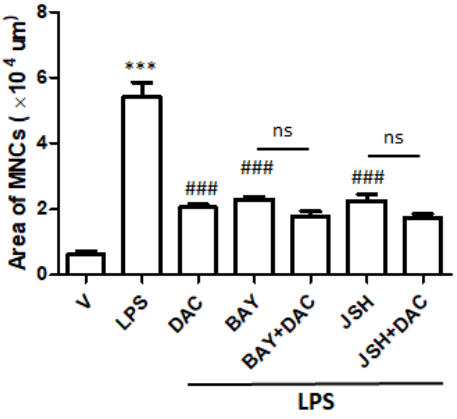
Area of MNCs (×10 4 um2)
8
6
4
2
0
***
###
###
###
ns
ns
V
LPS
DAC
BAY
BAY+DAC
JSH
JSH+DAC
LPS

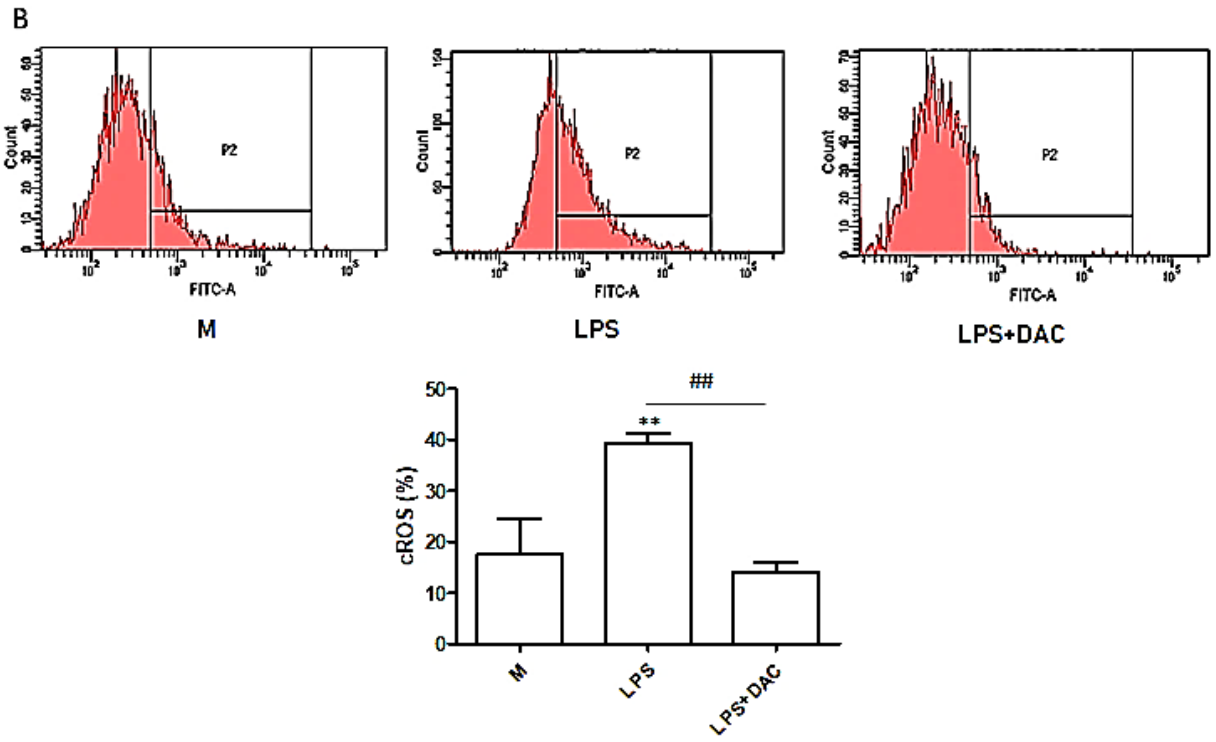
B
Count
P2
FITC-A
M
LPS
LPS+DAC
cROS (%)
##
**
M
LPS
LPS+DAC

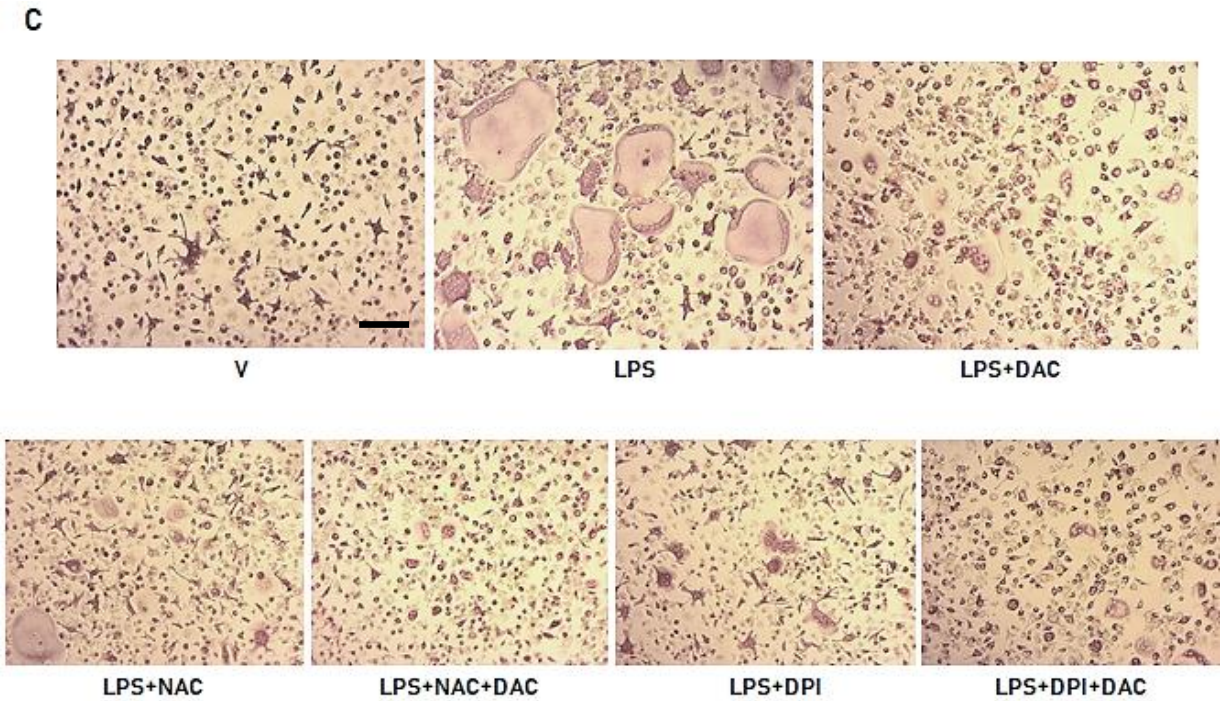
C
V
LPS
LPS+DAC
LPS+NAC
LPS+NAC+DAC
LPS+DPI
LPS+DPI+DAC

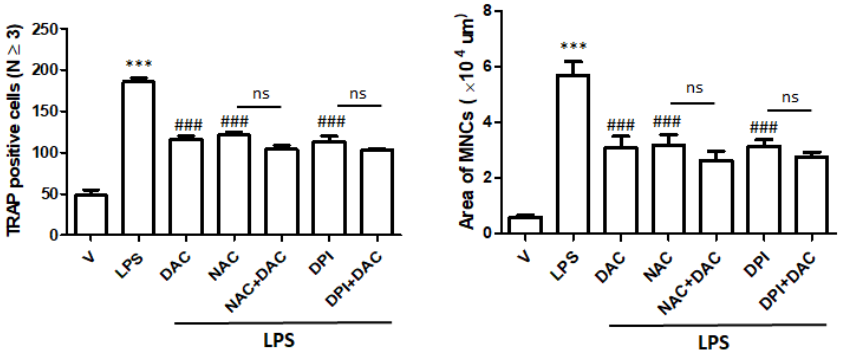
TRAP positive cells (N ≥ 3)
250
200
150
100
50
0
***
###
###
###
ns
ns
V
LPS
DAC
NAC
NAC+DAC
DPI
DPI+DAC
LPS
Area of MNCs (×10 4 um)
8
6
4
2
0
***
###
###
###
ns
ns
V
LPS
DAC
NAC
NAC+DAC
DPI
DPI+DAC
LPS

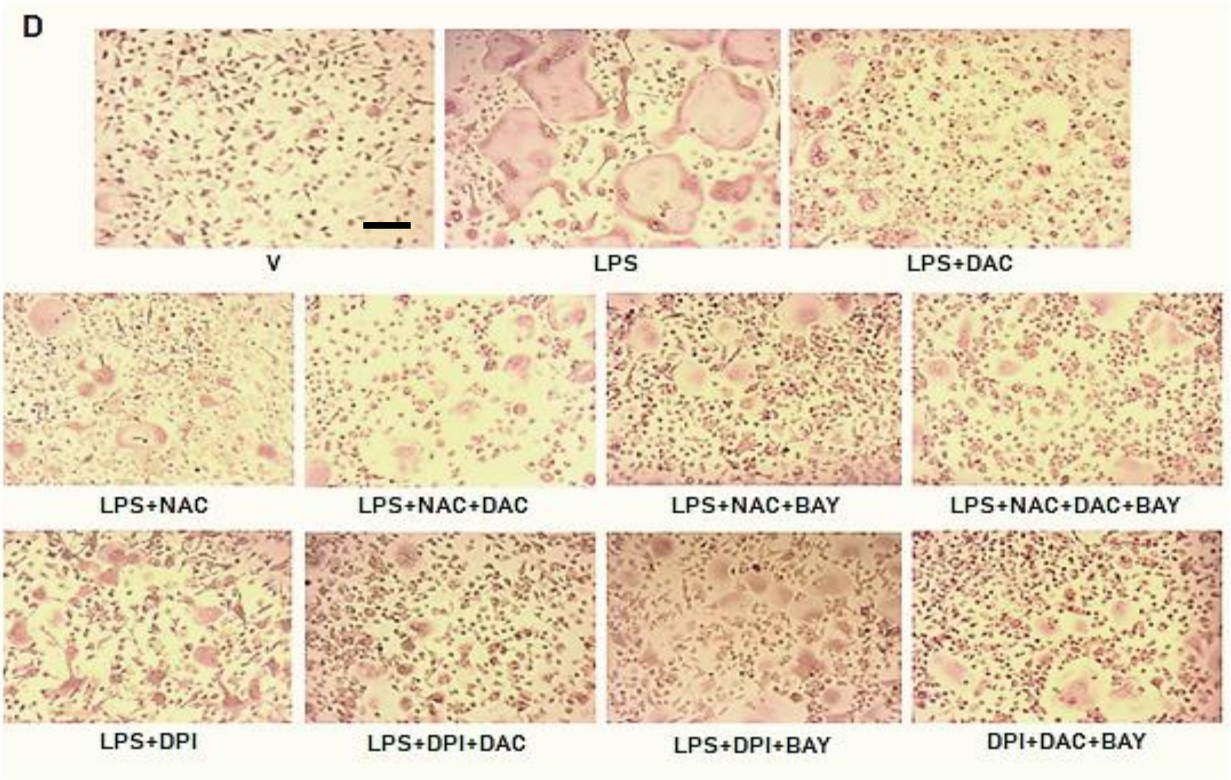
D
V
LPS
LPS+DAC
LPS+NAC
LPS+NAC+DAC
LPS+NAC+BAY
LPS+NAC+DAC+BAY
LPS+DPI
LPS+DPI+DAC
LPS+DPI+BAY
DPI+DAC+BAY

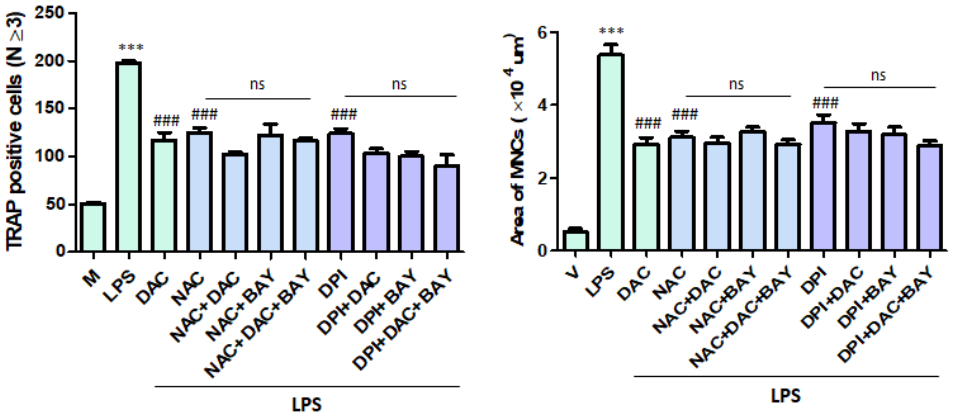
TRAP positive cells (N ≥3)
250
200
150
100
50
0
***
###
###
###
ns
ns
M
LPS
DAC
NAC
NAC+DAC
NAC+BAY
NAC+DAC+BAY
DPI
DPI+DAC
DPI+BAY
DPI+DAC+BAY
LPS
Area of MNCs (×10 4 um)
6
4
2
0
***
###
###
###
ns
ns
V
LPS
DAC
NAC
NAC+DAC
NAC+BAY
NAC+DAC+BAY
DPI
DPI+DAC
DPI+BAY
DPI+DAC+BAY
LPS

Figure 2. DAC treatment attenuates activation of NF-KB signaling and level of cytosolic reactive oxygen species (cROS) upon LPS treatment in Ocs.

Pre- osteoclasts incubated more in presence of BAY 11-7082 (3µM) or JSH-23 (10 µM) and stimulated with LPS (50 ng/ml) with or without DAC (7µM) for 48 h. After TRAP staining, the number and area of osteoclasts counted (A). The level of cytosolic ROS is measured by flow cytometry using H^2DCF-DA (B). The cells treated with DPI (5nM) or NAC (3mM) upon LPS stimulation in presence or absence of DAC (7µM) , Number and area of osteoclasts are represented (C). To assess the role of DAC in inhibition of both NF-KB activation and ROS, pre- osteoclasts are treated with co-treatment of NAC (3mM), DPI (5nM) and BAY 11-7082 (3µM) in presence or absence of DAC(7µM). After TRAP staining, the number and area of osteoclasta are measured (D). *** $p < 0.001$ compared with RANKL pre- treated cells as vehicle (V). ## $p < 0.01$; ### $p < 0.001$ compared with LPS treated cells. ns, no significant difference between 2 samples. Similar results were obtained in three

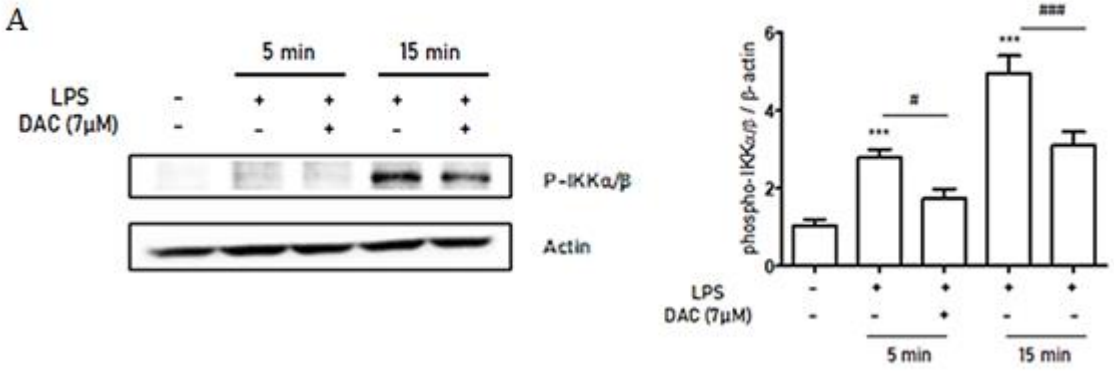
A
5 min
15 min
LPS
DAC (7μM)
P-IKKα/β
Actin
phospho-IKKα/β / β-actin
LPS
DAC (7μM)
5 min
15 min

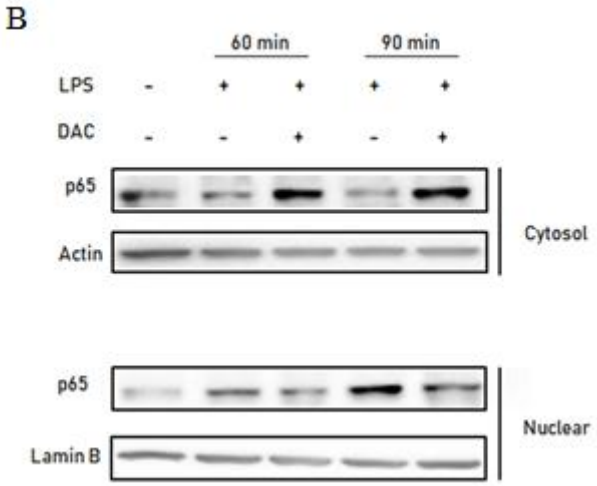
B
60 min
90 min
LPS
DAC
p65
Actin
Cytosol
p65
Lamin B
Nuclear

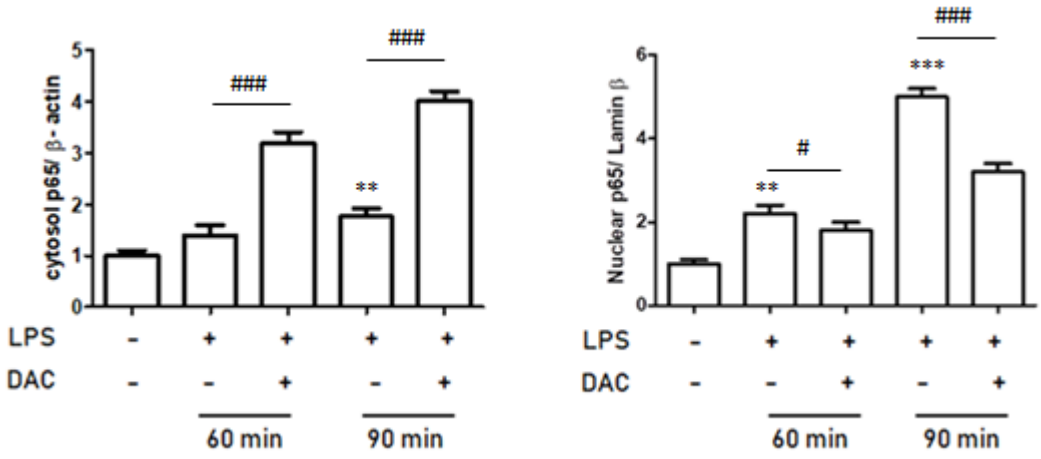
cytosol p65/ β- actin
LPS
DAC
60 min
90 min
Nuclear p65/ Lamin β
LPS
DAC
60 min
90 min

Figure 3. DAC decreases the NF- KB signaling and nuclear localization of p65 upon LPS stimulation

Whole cell extracts were subjected to western blot analysis to measure the phospho- IKKα/β level upon LPS stimulation in presence or absence of DAC (7μM) with an Ab against phospho- IKKα/β (A). After fractionation of cell extracts into cytoplasmic and nuclear parts, each was evaluated by Western blot analysis with antibodies against p65, and β-actin and lamin B1 for normalization for cytosol p65 and nuclear level respectively (B).

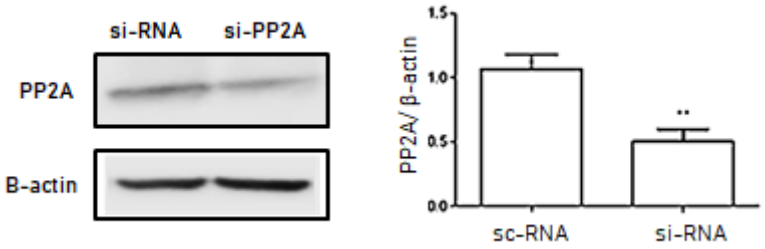
si-RNA
si-PP2A
PP2A
B-actin
PP2A/ β-actin
1.5
1.0
0.5
0.0
**
sc-RNA
si-RNA

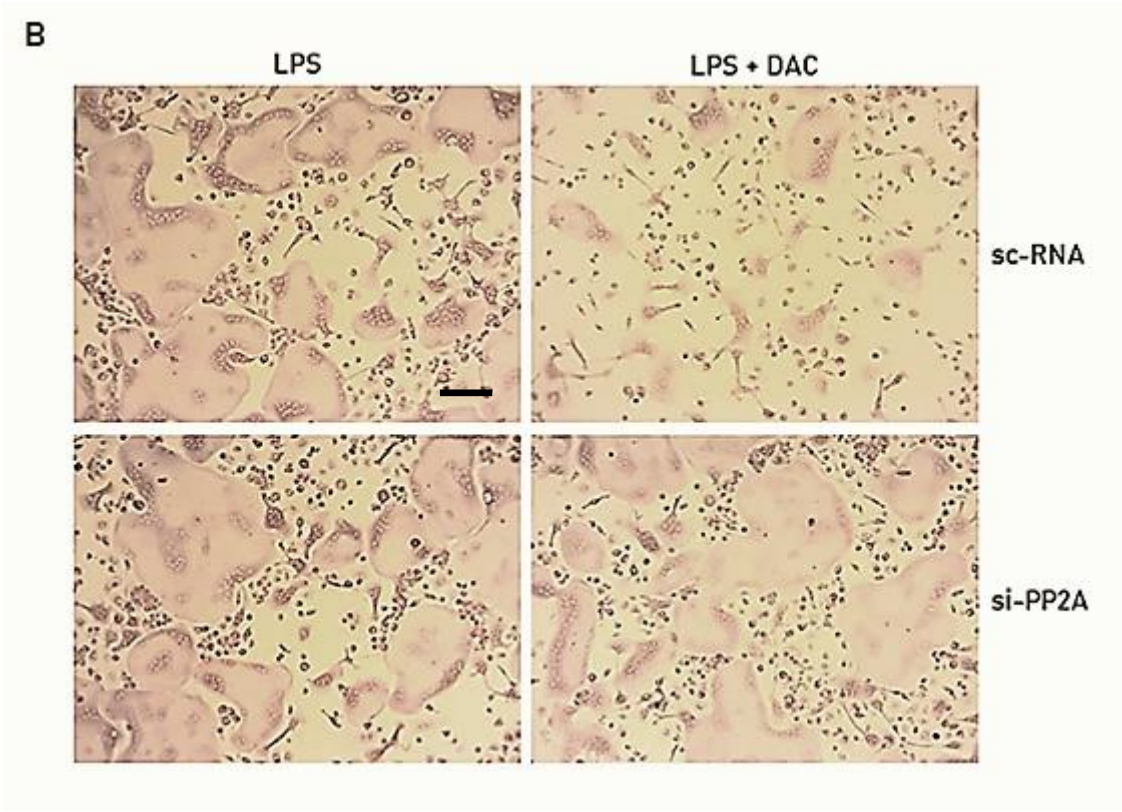
B
LPS
LPS + DAC
sc-RNA
si-PP2A

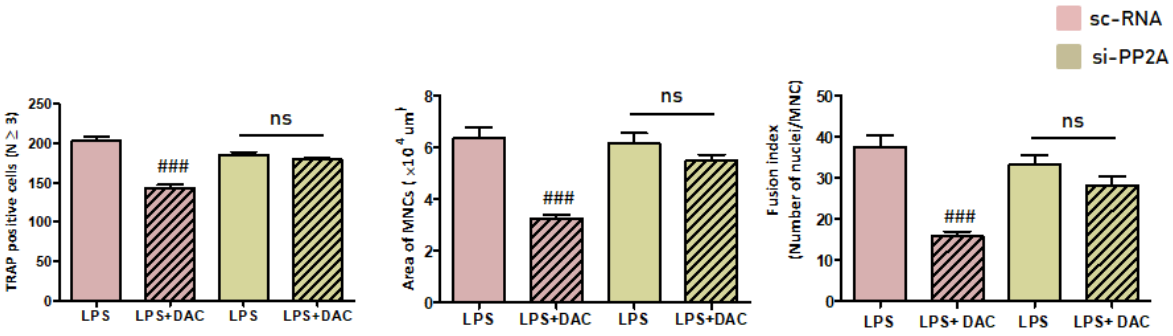
sc-RNA
si-PP2A
TRAP positive cells (N ≥ 3)
250
200
150
100
50
0
###
ns
LPS
LPS+DAC
LPS
LPS+DAC
Area of MNCs (×10 4 um 2)
8
6
4
2
0
###
ns
LPS
LPS+DAC
LPS
LPS+DAC
Fusion index (Number of nuclei/MNC)
50
40
30
20
10
0
###
ns
LPS
LPS+ DAC
LPS
LPS+ DAC

Figure 4. DAC decreases osteoclastogenesis upon LPS stimulation via PP2A

Cells were transfected with 50 nM of scRNA or siPP2A and further incubated with LPS and M-CSF with or without DAC (7μM), and after TRAP staining the number of TRAP-positive MNCs was counted. The area and fusion index of cells are represented as well (B). Reduced expression of PP2A by PP2A silencing was confirmed by western blot (A). ** $p < 0.01$; *** $p < 0.001$ compared with sc-RNA transfected cells. # $p < 0.05$; ## $p < 0.01$; ### $p < 0.001$ compared with LPS-treated cells. ns, no significant difference between 2 samples. Similar results were obtained in three independent experiments.

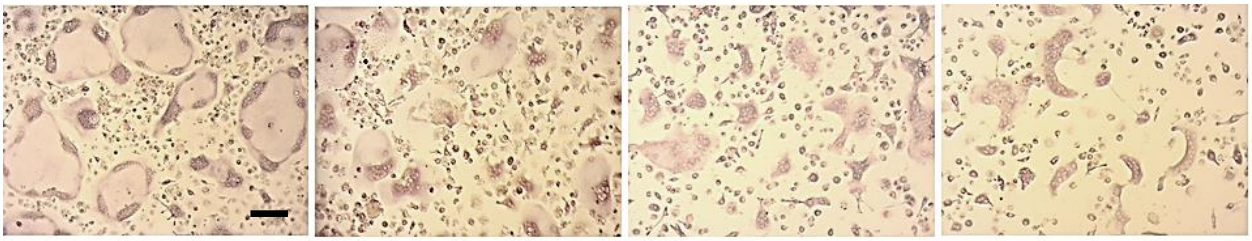
M+R
M+R+DAC.3 μM
M+R+DAC.5μM
M+R+DAC.7μM

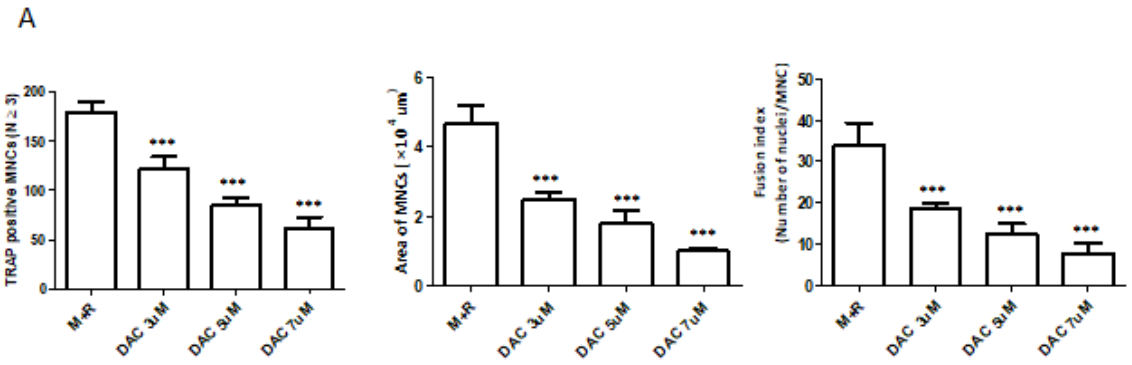
A
TRAP positive MNCs (N ≥ 3)
Area of MNCs (×10⁻⁴ um²)
Fusion index (Number of nuclei/MNC)
M+R
DAC 3uM
DAC 5uM
DAC 7uM

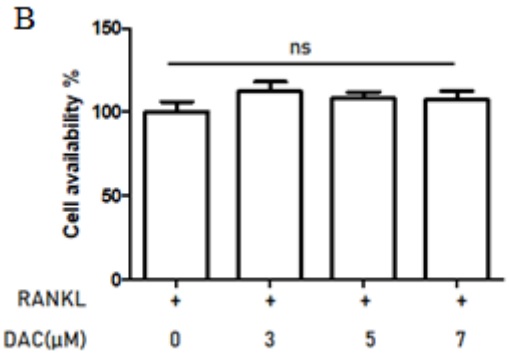
B
Cell availability %
ns
RANKL
DAC(μM)
0
3
5
7

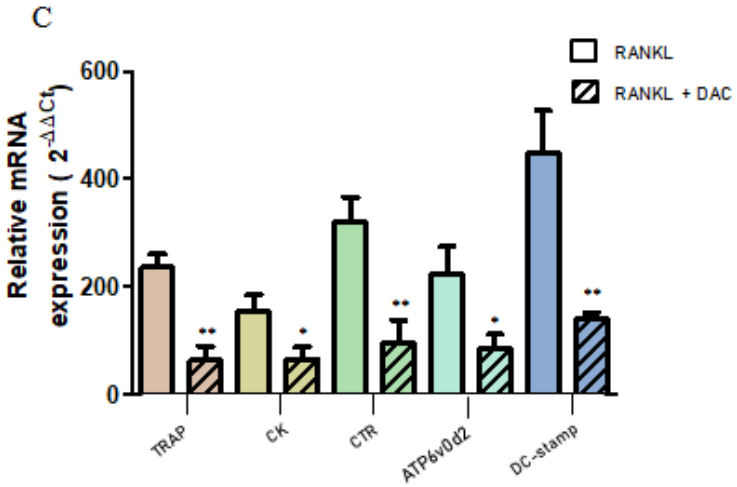
C
Relative mRNA expression (2-ΔΔCt)
RANKL
RANKL + DAC
TRAP
CK
CTR
ATP6v0d2
DC-stamp

Figure 5. DAC decreases the Differentiation of osteoclasts upon RANKL stimulation *in vitro*.

Bone marrow derived macrophages (BMMs) were further incubated with M-CSF (30 ng/mL) and RANKL (40 ng/mL) in presence or absence of DAC (3 μM, 5 μM, or 7 μM) (A, B, C). After fixation and TRAP staining, TRAP- positive multinucleated cells (MNCs) were counted. 70≥ cells were selected randomly for measuring the area and fusion index (average of nuclei number/ TRAP positive MNCs)(A). To measure the cell viability, MTT assay was used to compare the cells treated with different concentration of DAC with RANKL treated cells (B). qPCR was performed to check the effect of DAC (7μM) on RANKL- induced expression of genes specific to osteoclasts. The expression level is normalized to BMM cells (C). * $p < 0.05$; ** $p < 0.01$; *** $p < 0.001$ compared with RANKL- treated cells. ns, no significant difference between 2 samples. Similar results were obtained from three independent experiments.

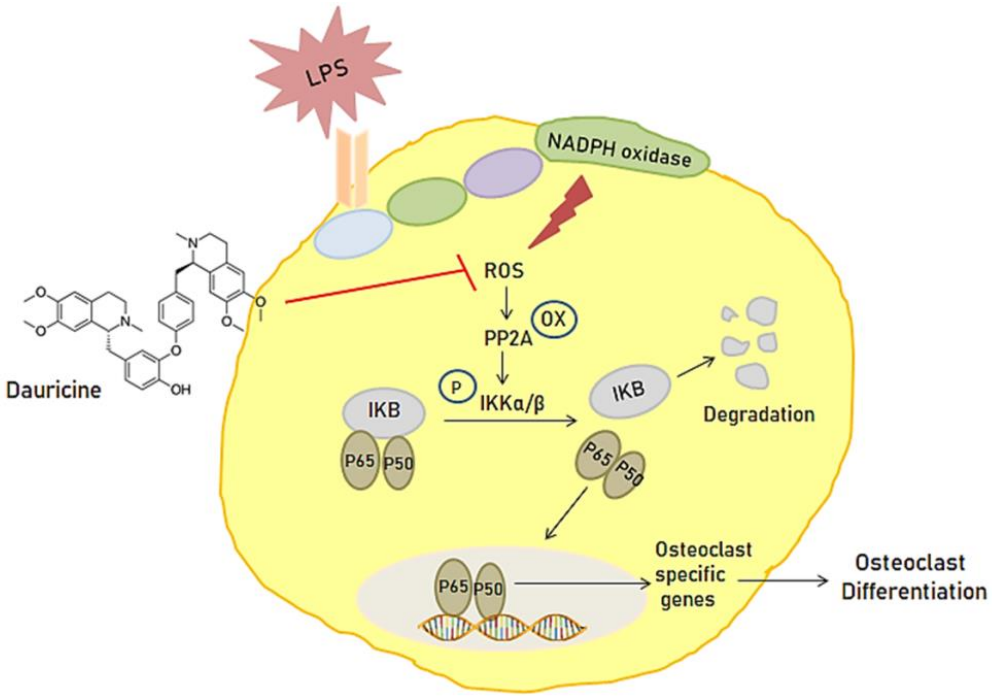
LPS
NADPH oxidase
ROS
PP2A
OX
P
IKKα/β
IKB
P65
P50
IKB
Degradation
P65
P50
P65
P50
Osteoclast
specific
genes
Osteoclast
Differentiation
Dauricine
OH

References used for ABSTRACT figure:

1. Jung, K. J.; Kim, D. H.; Lee, E. K.; Song, C. W.; Yu, B. P.; Chung, H. Y. Oxidative stress induces inactivation of protein phosphatase 2A, promoting proinflammatory NF-κB in aged rat kidney. Free Radical Biology and Medicine. 2013, 61, 206- 217.
2. Lee, T.; Shih, R. H.; Lin, C. C.; Chen, J. T.; Yang, C. M. Role of TLR4/NADPH oxidase/ROS-activated p38 MAPK in VCAM-1 expression induced by lipopolysaccharide in human renal mesangial cells. Cell communication and signaling. 2012, 10, 1- 15.

Chapter II

Estrogen protects against Ovariectomy- induced Bone loss in mice model via ERα/SHP2/c-Src Complex to Decrease Cytoskeletal Organization of Osteoclasts

1. Introduction

Bone remodeling serves to regulate bone architecture needed for mechanical changes and it helps to repair microdamages in bone matrix and prevents the accumulation of old bone. Imbalance between bone formation and bone resorption will lead to inappropriate bone remodeling and osteoporosis [1]. Postmenopausal osteoporosis is a systemic metabolic bone disease with low bone mass and micro fractures in bone tissue upon loss of ovarian function.

Estrogen deficiency has been associated with higher differentiation and function of osteoclasts (OCs) and is one of the most common reasons of postmenopausal osteopororsis [2, 3]. Although E2 has been demonstrated to be involved in prevention of bone resorption [3,4], but the detailed mechanisms are not clear and remain to investigate.

Previous studies have shown E2/ estrogen receptor (ER) signaling mediates apoptosis of OC to reduce bone resorption [5, 6]. It has been reported that the phenotype of ERα-knock out (KO) mice is similar to that of osteoporotic women with low trabecular bone density caused by high bone resorption and decreased apoptosis of OCs [7], suggesting that ERα is necessary to protect trabecular bone via OCs. Not only, ERs can regulate the expression of target genes through binding to their specific response elements but also they can transmit the signals in non-genomic way [8- 10]. E2 shows cellular responses in a non-nuclear manner via it´s receptors present at the cell membrane and cytoplasm [8]. Differentiation and survival of osteoclast is critical for their bone matrix degradation activity which is mainly controlled by cytoskeletal organization.

Deliver of Lysosome- derived vesicles carrying protons, chlorides and cathepsin K to plasma membrane in resorption area is important for ruffled border formation and bone degradation [11]. The bone degradation activity of mature OCs is mainly controlled by the cytoskeletal organization of an actin ring surrounding the resorption area to isolate it from the extracellular space and centralize bone-degrading molecules.

Integrin αVβ3 mediates the differentiation and function of osteoclasts to polarize and degrade bone and it´s deficiency has been resulted in impaired cytoskeleton and bone reasorption leading to higher bone mass [12]. Similar phenotype is observed in the absence of c-Src demonstrating impaired cytoskeletal organization in osteoclasts [13]. RANKL induces c-Src/Vav3 to associate with RANK in an αvβ3- dependent manner leading to activation of Rac1 and subsequent bone resorption[14, 15, 16]. In the presence of RANKL, RANK and αvβ3 integrin contribute in signaling complex via direct binding of SH3 domain of c-Src and β-cytoplasmic tails of αvβ3 integrins leading to an integrin-associated canonical pathway for actin ring formation via an axis of c-Src/Vav3/Rac1.

In this study, we have investigated a signaling pathway of E_2 to decrease RANKL-stimulated cytoskeletal organization and subsequent bone resorption.

2. Material and Methods

2.1. Ethics Statement

All mice experiments were followed by guidelines of the Institutional Animal Care and Committee of the Immunomodulation Research Center (IRC), University of Ulsan. The approval ID for this study is #HSC-19–010 (20190801).

2.2. Reagents and Antibodies

Recombinant mouse macrophage-colony stimulating factor (M-CSF) and receptor activator of nuclear factor κB ligand (RANKL) were acquired from R and D Systems, Inc. (Minneapolis, MN, USA). Estradiol, 20 ,20 ,20 –tribromoethanol was from Sigma Chemicals (St. Louis, MO, USA). MPPD was obtained Tocris (Bristol, UK). Minimum essential medium α (α-MEM) without phenol red was from Life Technologies (Carlsbad, CA, USA). c-Src-Y416 was from Cell Signaling Technology (Denver, MA, USA); c-Src homology 2 (SH2) containing protein tyrosine phosphatase 2 (SHP2), estrogen receptor α (ERα), and caveolin-1 were received from Santa Cruz Biotechnology (Santa Cruz, CA, USA). c-Src and β-actin were from ECM Biosciences and Sigma-Aldrich (St. Louis, MO, USA) respectively.

2.3. Animals, cell culture and osteoclast differentiation

Sham (n= 10) and ovariectomy (n=12) surgery are performed under anesthesia on ten week old female mice of C57BL/6J strain. 2 days after surgery, the mices injected intraperitoneally (i. p) with E2 (0.1mg/kg) or Vehicle daily for 4 weeks. To identify osteoclasts positive for TRAP *in vivo*, mouse femora were dissected and after removing the tissue, decalcified with EDTA and subjected to TRAP staining. 4 groups were stained for TRAP to identify OCs (original magnification x400).

To get the bone marow cells, after removing the Femora and tibiae and dissection of adherent soft tissue, the ends of bone were cut and flushed with α-MEM using a sterile 21-gauge needle. The

cells incubated for with 16 hours treated with M-CSF (20 ng/ml). To get the adherent monocyte/ macrophage- like cells, non-adherent cells harvested and cultured for more 2 days [17] which were analyzed to be negative for CD3 and CD45R and positive for CD115 [18]. The cells are treated with M-CSF and RANKL (40 ng/ml) and medium was replaced on day 2 followed by culturing the cells in α-MEM without phenol red containing 10% charcoal-treated FBS [19] for E_2 treatment *in vitro.* The cells fixed in 10% formalin for 10 min and stained for TRAP as described [17]. The number and area of TRAP-positive multinucleated cells (MNC) with three or more nuclei were analyzed and fusion index was represented as the average number of nuclei per for TRAP positive osteoclasts [20].

2.4. RNA Isolation and Quantitative Polymerase Chain Reaction (qPCR)

Total RNA was isolated using QIAzol reagent and first-strand cDNA was reverse transcribed with random primers and Moloney murine leukemia virus (M-MLV) reverse transcriptase as described in Park et al. [17]. qPCR was performed using SYBR green real-time PCR master mixes and primers related to genes (TRAP, NFAT2, cathepsinK). Relative gene expression was calculated using the formula $2^{-\Delta\Delta Ct}$ normalized to housekeeping gene, ribosomal protein small subunit (RPS) [18]. The primer sequences were used as described in previous research [17].

Gene name	Forward sequence 5´- 3´	Reverse sequence 5´- 3´
Cathepsin K	GGGCCAGGATGAAAGTTGTA	CACTGCTCTCTTCAGGGCTT
NFAT2	AATAACATGCGAGCCATCATC	TCACCCTGGTGTTCTTCCTC
TRAP	GACCACCTTGGCAATGTCTCTG	TGGCTGAGGAAGTCATCTGAGTTG
RPS	ATCAGAGAGTTGACCGCAGTTG	AATGAACCGAAGCACACCATAG

2.5.Cell viability

To evaluate the cell viability, After differentiation, the cells were washed and incubated for 3 hr with MTT (3-(4,5-dimethylthiazol-2-yl)-2,5-diphenyltetrazolium bromide) at 37℃. After removal of MTT, reduced MTT crystals (formazan) dissolved in DMSO (Dimethyl sulfoxide), resulting in colored solution. The absorbance was measured at 540 nm with a microplate reader.

2.6. Western Blot Analysis

Cell lysates were subjected to protein extraction using lysis buffer (50 mM Tris-HCl, pH 8.0, 150 mM NaCl, 1 mM EDTA, 0.5% Nonidet P-40, 0.01% protease inhibitor mixture). After using bicinchoninic acid (BCA) assay to detect protein concentration, 20 µg of total protein were subjected to sodium dodecyl sulfate–polyacrylamide gel electrophoresis (SDS–PAGE) and subsequent transfer onto nitrocellulose membranes. Skim milk (5%) in Tris-buffered saline containing 0.1% Tween-20% used for blocking of the membrane which is then incubated overnight at 4 ◦C [17] with antibodies (Ab) against c-Src-Y416, c-Src, ERα, caveoline and β-actin. The lysate (200 µg) was subjected to immunoprecipitation with 1 µg of antibody against ERα, c-Src, or SHP2, followed by Western blot analysis using the corresponding Ab as indicated in the figures.

2.7.Detection of Oxidized SHP2 by Carboxymethylation

BMMs were treated with or without E2 (5nM) after incubation with M-CSF (30 ng/mL) and RANKL (40 ng/mL) for 55 h for 16 h. The medium was removed, and the cells were frozen rapidly in liquid nitrogen. The cells were transferred to 100 µM N-(biotinoyl)-N0 -(iodoacetyl) ethylenediamine (BIAM)-containing lysis buffer (50 mM Tris-HCl, pH 7.5, 150 mM NaCl, 0.5% Triton X-100, 10 µg/mL aprotinin, and 10 µg/mL leupeptin; rendered oxygen-free by bubbling nitrogen gas through the buffer at a low flow rate for 20 min). Sulfhydryl modifying chemical BIAM selectively detects the reduced form of cysteine [20]. Next, after centrifugation, the samples subjected to immunoprecipitation with 1 µg of Ab against SHP2. HRP-conjugated streptavidin was used to detect the immunocomplexes labeled with BIAM and the color was developed with an enhanced chemiluminescence kit.

2.8. Bone Resorption

The bone resorption activity of OCs were assessed by culturing the mature osteoclasts on dentine slices as described in a previous report [17]. To explain in more details, Macrophage/ Monocyte like cells incubated with M-CSF (30 ng/mL) and RANKL (40 ng/mL) to get the mature osteoclasts. The multi- nuclear Cells are seeded on dentine slices and further incubated with E2 or MPPD for 3 days. The cells were subjected to TRAP staining and after removing the cells via ultrasonication in 1 M NH4OH, the dentine slices were stained with 1% (w/v) toluidine blue in 0.5% sodium borate to visualize resorption pits. ImageJ software, 1.37v was used to measure the resorbed areas.

2.9. Statistical Analysis

Values are expressed as means of triplicate experiments ± standard deviation (SD). Each series of experiments was repeated at least three times. For comparison between 2 groups, Student's t-test was performed. Two-way analysis of variance (ANOVA) was performed when two variables were analyzed. A p-value of less than 0.05 was considered statistically significant.

3. Results

3.1. E2 Decreases osteoclastogenesis during induced Bone Loss in OVX Mice model

To investigate the role of E2 on osteoclastogenesis in OVX-induced bone loss we evaluated the effect of E2 on OCs from E2-injected OVX mice. In vivo, TRAP-staining showed that E2 significantly decreased OC surface area (OC.S/BS), which increased after 4 weeks of OVX (Figure 1A) without affecting the body weight and food intake significantly (Figure 1B).

3.2. E2 decrease Number and Size of OCs during Osteoclast Differentiation in vitro

To investigate the effect of E2 on OC differentiation in vitro, we checked the expression of OC-specific genes induced by RANKL after 48 h of treatment with E2. E2 exposure did not change the expression level of specific genes included of TRAP, nuclear factors of activated T cells 2 (NFAT2) and the lysosomal proteolytic enzyme cathepsin K [2,3] as shown in figure 2A.

To assess the effect of E2 in the late stage of osteoclast differentiation, we treated the osteoclast with E2 after 55 hours first exposure of RANKL. E2 decreased significantly the number, area and fusion index in dose dependent manner while the effect on area was higher comparing to number and nuclei number (Figure 2B).

To investigate whether the effect of E2 is related to M-csf or RANKL, cells were treated with M-csf or RANKL or both of them in presence or absence of E2. While there was no effect on M-csf signaling, E2 mitigated the RANKL signaling significantly (Figure 2C). In reverse, MPPD which is the antagonist of ERα receptor, increased the area and fusion index significantly without affecting the number of osteoclasts (Figure 2C).

3.3 E2 attenuated bone resorption activity of osteoclast upon RANKL signaling

To assess the effect of E2 on cell viability in the late stage of osteoclast differentiation, we treated the osteoclast with E2 after 55 hours first exposure of RANKL and after differentiation, MTT assay was performed. The different concentartion of E2 (1nM, 5nM and 10nM) did not affected the cell viability (figure 3A). To investigate the effect of E2 on survival of osteoclast after maturation is related to M-CSF or RANKL signaling, after maturation, the cells were washed and treated more in defined conditions. E2 decreased the survival of osteoclasts upon RANKL treatment while there is no significant difference upon M-CSF or both co- treatment of M-CSF and RANKL in presence or absence of E2 (figure 3B). To assess the effect of E2 on bone resorption activity of osteoclasts we cultured mature osteoclast on dentine slices treated with E2 or MPPD. E2 attenuated the resorbed area (total pit area/OC number) while MPPD significantly increased the activity of osteoclast in bone resorption (figure 3C).

3.4. E2 disrupts c-Src activation in a Non-Genomic Manner

Based on previous results, E2 inhibited RANKL-induced actin ring formation in Ocs. Next, we assessed how E2 can affect RANKL signaling that regulate cytoskeletal organization of osteoclasts.

Interaction between ERα and caveolin-1, a plasma membrane marker that can induce the nuclear translocation, did not show any significant change in presence or absence of E2 exposure (figure 4A). Further, to evaluate the effect of E2 on RANKL signaling we checked phosphorylation of c-Src (c-Src-Y416) as activated form. Previously, it has been reported that E2 transmits signals through genomic and non-genomic mechanisms [22-24]. As shown in figure 4B, E2 mitigated significantly the phosphorylation of c-Src as early as 1 min exposure of E2. While , MPPD, the antagonist of ERα, increased the phosphorylation level of c-Src. All together, E2 attenuated RANKL- induced osteoclastogenesis and cytoskeleton organization in non-genomic way.

3.5. E2 Inhibits RANKL-Induced Cytoskeletal Reorganization via an complex of ERα/c-Src/SHP2 Leading to Decreased VAV3 activation

To assess the molecular function of E2 in regulating activation of c-Src upon RANKL signaling, co- immunoprecipitation showed enhanced interaction between ERα and c-Src in case of E2 exposure, whiles, MPPD, attenuated the interaction (figure 5A). It has been confirmed Tyrosine phosphatase is required to reduce c-Src signaling and SHP2 is associated physically with ERα [23], so we checked how it will be modulated in case of E2 exposure in RANKL- induced osteoclastogenesis. E2 exposure increased the association between SHP2 and ERα while MPPD resulted in opposite (figure 5A). Next, we investigated whether decreased c-Src activation is transmitted to block phosphorylation of Vav3 which is responsible for Rac1activation to affect actin ring formation. Vav3 has been reported to be an OCspecific guanidine nucleotide exchange factor that targets Rac1 [25]. Consistent with its effect on c-Src, E2 attenuated the tyrosine phosphorylation of Vav3 induced by RANKL while in reverse MPPD increased the phosphorylation level (figure 5B).

4. Discussion

In this study, we found the non-genomic effect of E2 on osteoclast to protect bone from OVX-induced bone loss. Expression level of genes specific to osteoclasts remained unchange in presence of E2 implying early stage of osteoclast differentiation is not modulated by E2. Based on in vivo and in vitro TRAP staining, area is affected more dramatic comapring with number and fusion index of osteoclast. In contrast, MPPD, ERα antagonist, increased the area of osteoclast, suggesting that E2/ ERα signaling may affect the cytoskeletal reorganization of osteoclasts in non- genomic way.

As shown in results, actin ring formation was disrupted by E2 exposure upon RANKL signaling not M-CSF stimulation. Our data suggested that E2 effect on osteoclasts is dependent on RANKL signaling and subsequent c-Src activation to block actin ring formation [9].

E2 could decrease the level of phosphorylated c-Src-Y416 even after 1 min exposure, suggesting the signaling via E2 is rapid. Further, co-immunoprecipitation assay showed the interaction between ERα and caveolin-1 which is a plasma membrane marker representing ERα is located on plasma membranes.

The results indicated that inhibitory effect of E2 on c-Src activation upon RANKL signaling happened in non genomic way. Not only ERs are nuclear receptors with the ability to regulate the expression of genes via specific response elements in DNA, but also, they have secondary signaling in non- genomic way [22-24]. As confirmed by our data also, E2 showed cellular responses in non-nuclear manner through receptors found in cell membranes [22].

E2 displayed the protective effect in bone loss through acting on osteoclasts [26, 27]. In mice model also specific ERα- knockout in osteoclasts showed same phenotype as osteoporotic women with low bone mass [27]. Mature osteoclasts with knockout of ERα showed resistance against

apoptosis effects of E2 indicating the effect of E2 increasing the bone mass is related to apoptosis of osteoclasts [27-29].

In our results E2 displayed the effect on cytoskeletal organization rather than the number of osteoclasts confirming previous studies [30, 31]. Kameda and colleagues showed E2 can affect the cytoskeletal organization via Siglec-15 in osteoclasts preventing their spread needed for bone loss [30]. In the study performed by Kajiya and colleagues, Genistein, a phytoestrogen, impaired actin ring formation and subsequent bone resorption activity of osteoclasts by increasing cytosolic level of Ca2+ [31]. In our study, we showed the molecular pathway of E2 to impair the actin ring formation leading to less bone resorption activity.

We demonstrated the detailed molecular mechanism of how E2 disrupted cytoskeletal reorganization in OCs. E2 increased the association between c-Src and reduced form of SHP2 which is the activated form. As shown in the result of co-immunoprecipitation, E2/ ERα interaction will lead to a complex with c-Src and SHP2 followed by dephosphorylation of Y416 of c-Src. The coupling of ERα with both SHP2 and c-Src impaied the signal stimulated by RANKL.

The experiments carried by immunoprecipitation, carboxymethylation, and ROS level showed that RANKL stimulation increased a direct interaction between NOX1 and SHP2 which is inactived by ROS-induced oxidation, whereas E2 treatment showed the reverse results.

In summary, E2/ ERα signaling will lead to formation of a complex with active SHP2 and c-Src due to available SHP2 because of less interaction with NOX1. The complex will lead to decreased c-Src activation upon RANKL signaling.

In spite of strong effect on postmenopausal osteoporosis, the usage of E2 as therapeutic agent is limited because of side effects [33]. As shown in our data, SHP2 or NOX1 acted as downstream target of E2 to disrupt actin ring formation in osteoclasts. Now, there are some SHP2 inhibitors under

considerations as therapies for tumor [34] and NAC, a ROS scavenger has been shown to be effective to ameliorate traumatic brain injury in human [35] introducing them as alternative agents to E2 to prevent bone loss in human.

5. Conclusion

In general our data demonstrated that E2/ ERα binding will lead to a complex with SHP2 and c-Src. Due to less interaction between NOX1 and inactive form of SHP2, RANKL- induced c-Src activation and subsequent cytoskeletal organization in non genomic way. Dephosphorylation of c-Src upon E2c exposure will lead to blockage of Vav3 and Rac1 which are mediators in RANKL- induced actin ring formation and bone resorption (Figure 6). We could identify the function of E2 on osteoclast disrupting actin ring formation in non- genomic way and importance of SHP2 and NOX1 as therapeutic targets in case of osteoporosis upon estrogen deficiency.

References

1. Raisz, L.G. Pathogenesis of osteoporosis: Concepts, conflicts, and prospects. J. Clin. Investig. 2005, 115, 3318–3325.
2. Feng, X.; Teitelbaum, S.L. Osteoclasts: New Insights. Bone Res. 2013, 1, 11–26.
3. Boyle, W.J.; Simonet, W.S.; Lacey, D.L. ; Osteoclast differentiation and activation. Nature 2003, 423, 337–342.
4. Teitelbaum, S.L. Osteoclasts: What do they do and how do they do it? Am. J. Pathol. 2007, 170, 427–435.
5. McHugh, K.P.; Hodivala-Dilke, K.; Zheng, M.H.; Namba, N.; Lam, J.; Novack, D.; Feng, X.; Ross, F.P.; Hynes, R.O.; Teitelbaum, S.L. Mice lacking beta3 integrins are osteosclerotic because of dysfunctional osteoclasts. J. Clin. Investig. 2000, 105, 433–440.
6. Soriano, P.; Montgomery, C.; Geske, R.; Bradley, A. Targeted disruption of the c-src proto-oncogene leads to osteopetrosis in mice. Cell 1991, 64, 693–702.
7. Faccio, R.; Novack, D.V.; Zallone, A.; Ross, F.P.; Teitelbaum, S.L. Dynamic changes in the osteoclast cytoskeleton in response to growth factors and cell attachment are controlled by beta3 integrin. J. Cell Biol. 2003, 162, 499–509.
8. Croke, M.; Ross, F.P.; Korhonen, M.; Williams, D.A.; Zou, W.; Teitelbaum, S.L. Rac deletion in osteoclasts causes severe osteopetrosis. J. Cell Sci. 2011, 124, 3811–3821.
9. Izawa, T.; Zou, W.; Chappel, J.C.; Ashley, J.W.; Feng, X.; Teitelbaum, S.L. c-Src links a RANK/αvβ3 integrin complex to the osteoclast cytoskeleton. Mol. Cell Biol. 2012, 32, 2943–2953..
10. Rachner, T.D.; Khosla, S.; Hofbauer, L.C. Osteoporosis: Now and the future. Lancet 2011, 377, 1276–1287.
11. Manolagas, S.C. From estrogen-centric to aging and oxidative stress: A revised perspective of the pathogenesis of osteoporosis. Endocr. Rev. 2010, 31, 266–300.

12. Selby, P.L.; Peacock, M.; Barkworth, S.A.; Brown, W.B.; Taylor, G.A. Early effects of ethinyloestradiol and norethisterone treatment in post-menopausal women on bone resorption and calcium regulating hormones. Clin. Sci. 1985, 69, 265–271.
13. Ke, K.; Sul, O.J.; Rajasekaran, M.; Choi, H.S. MicroRNA-183 increases osteoclastogenesis by repressing heme oxygenase-1. Bone 2015, 81, 237–246.
14. Arai, F.; Miyamoto, T.; Ohneda, O.; Inada, T.; Sudo, T.; Brasel, K.; Miyata, T.; Anderson, D.M.; Suda, T. Commitment and differentiation of osteoclast precursor cells by the sequential expression of c-Fms and receptor activator of nuclear factor kappaB (RANK) receptors. J. Exp. Med. 1999, 190, 1741–1754.
15. De Faria, A.N.; Zancanela, D.C.; Ramos, A.P.; Torqueti, M.R.; Ciancaglini, P. Estrogen and phenol red free medium for osteoblast culture: Study of the mineralization ability. Cytotechnology 2016, 68, 1623–1632.
16. Okayasu, M.; Nakayachi, M.; Hayashida, C.; Ito, J.; Kaneda, T.; Masuhara, M.; Suda, N.; Sato, T.; Hakeda, Y. Low-density lipoprotein receptor deficiency causes impaired osteoclastogenesis and increased bone mass in mice because of defect in osteoclastic cell-cell fusion. J. Biol. Chem. 2012, 287, 19229–19241.
17. Park, H.J.; Son, H.J.; Sul, O.J.; Suh, J.H.; Choi, H.S. 4-Phenylbutyric acid protects against lipopolysaccharide-induced bone loss by modulating autophagy in osteoclasts. Biochem. Pharmacol. 2018, 151, 9–17.
18. De Jonge, H.J.M.; Fehrmann, R.S.N.; de Bont, E.S.J.; Hofstra, R.M.W.; Gerbens, F.; Kamps, W.A.; de Vries, E.G.E.; van der Zee, A.G.J.; te Meerman, G.J.; ter Elst, A. Evidence Based Selection of Housekeeping Genes. PLoS ONE 2007, 2, e898.
19. Kim, H.J.; Zhao, H.; Kitaura, H.; Bhattacharyya, S.; Brewer, J.A.; Muglia, L.J.; Ross, F.P.; Teitelbaum, S.L. Glucocorticoids suppress bone formation via the osteoclast. J. Clin. Investig. 2006, 116, 2152–2160.

20. Giannoni, E.; Buricchi, F.; Raugei, G.; Ramponi, G.; Chiarugi, P. Intracellular reactive oxygen species activate Src tyrosine kinase during cell adhesion and anchorage-dependent cell growth. Mol. Cell Biol. 2005, 25, 6391–6403.

21. Park, H.J.; Gholam-Zadeh, M.; Suh, J.H.; Choi, H.S. Lycorine Attenuates Autophagy in Osteoclasts via an Axis of mROS/TRPML1/TFEB to Reduce LPS-Induced Bone Loss. Oxid. Med. Cell Longev. 2019, 8982147.

22. Puglisi, R.; Mattia, G.; Carè, A.; Marano, G.; Malorni, W.; Matarrese, P. Non-genomic Effects of Estrogen on Cell Homeostasis and Remodeling With Special Focus on Cardiac Ischemia/Reperfusion Injury. Front. Endocrinol. 2019, 10, 1–18.

23. He, Z.; Zhang, S.S.; Meng, Q.; Li, S.; Zhu, H.H.; Raquil, M.A.; Alderson, N.; Zhang, H.; Wu, J.; Rui, L.; et al. Shp2 Controls Female Body Weight and Energy Balance by Integrating Leptin and Estrogen Signals. Mol. Cell Biol. 2012, 32, 1867–1878.

24. Haynes, M.P.; Li, L.; Sinha, D.; Russell, K.S.; Hisamoto, K.; Baron, R.; Collinge, M.; Sessa, W.C.; Bender, J.R. Src kinase mediates phosphatidylinositol 3-kinase/Akt-dependent rapid endothelial nitric-oxide synthase activation by estrogen. J. Biol. Chem. 2003, 278, 2118–2123.

25. Faccio, R.; Teitelbaum, S.L.; Fujikawa, K.; Chappel, J.; Zallone, A.; Tybulewicz, V.L.; Ross, F.P.; Swat, W. Vav3 regulates osteoclast function and bone mass. Nat. Med. 2005, 11, 284–290.

26. Lean, J.M.; Davies, J.T.; Fuller, K.; Jagger, C.J.; Kirstein, B.; Partington, G.A.; Urry, Z.L.; Chambers, T.J. A crucial role for thiol antioxidants in estrogen-deficiency bone loss. J. Clin. Investig. 2003, 112, 915–923.

27. Martin-Millan, M.; Almeida, M.; Ambrogini, E.; Han, L.; Zhao, H.; Weinstein, R.S.; Jilka, R.L.; O'Brien, C.A.; Manolagas, S.C. The estrogen receptor-alpha in osteoclasts mediates the protective effects of estrogens on cancellous but not cortical bone. Mol. Endocrinol. 2010, 24, 323–334.

28. Kameda, T.; Mano, H.; Yuasa, T.; Mori, Y.; Miyazawa, K.; Shiokawa, M.; Nakamaru, Y.; Hiroi, E.; Hiura, K.; Kameda, A.; et al. Estrogen inhibits bone resorption by directly inducing apoptosis of the bone-resorbing osteoclasts. J. Exp. Med. 1997, 186, 489–495.

29. Hughes, D.E.; Dai, A.; Tiffee, J.C.; Li, H.H.; Mundy, G.R.; Boyce, B.F. Estrogen promotes apoptosis of murine osteoclasts mediated by TGF–β. Nat. Med. 1996, 2, 1132–1136.

30. Kameda, Y.; Takahata, M.; Mikuni, S.; Shimizu, T.; Hamano, H.; Angata, T.; Hatakeyama, S.; Kinjo, M.; Iwasaki, N. Siglec-15 is a potential therapeutic target for postmenopausal osteoporosis. Bone 2015, 71, 217–226.

31. Kajiya, H.; Okabe, K.; Okamoto, F.; Tsuzuki, T.; Soeda, H. Protein tyrosine kinase inhibitors increase cytosolic calcium and inhibit actin organization as resorbing activity in rat osteoclasts. J. Cell Physiol. 2000, 183, 83–90.

32. Lee, N.K.; Choi, Y.G.; Baik, J.Y.; Han, S.Y.; Jeong, D.; Bae, Y.S.; Kim, N.; Lee, S.Y. A crucial role for reactive oxygen species in RANKL-induced osteoclast differentiation. Blood 2005, 106, 852–859.

33. Stepan, J.J.; Hruskova, H.; Kverka, M. Update on Menopausal Hormone Therapy for Fracture Prevention. Curr. Osteoporos. Rep. 2019, 17, 465–473.

34. Song, Z.; Wang, M.; Ge, Y.; Chen, X.P.; Xu, Z.; Sun, Y.; Xiong, X.F. Tyrosine phosphatase SHP2 inhibitors in tumor-targeted therapies. Acta Pharmacol. Sin. B 2021, 11, 13–29.

35. Bhatti, J.; Nascimento, B.; Akhtar, U.; Rhind, S.G.; Tien, H.; Nathens, A.; da Luz, L.T. Systematic Review of Human and Animal Studies Examining the Efficacy and Safety of N-Acetylcysteine (NAC) and N-Acetylcysteine Amide (NACA) in Traumatic Brain Injury: Impact on Neurofunctional Outcome and Biomarkers of Oxidative Stress and Inflammation. Front. Neurol. 2017, 8, 744.

A

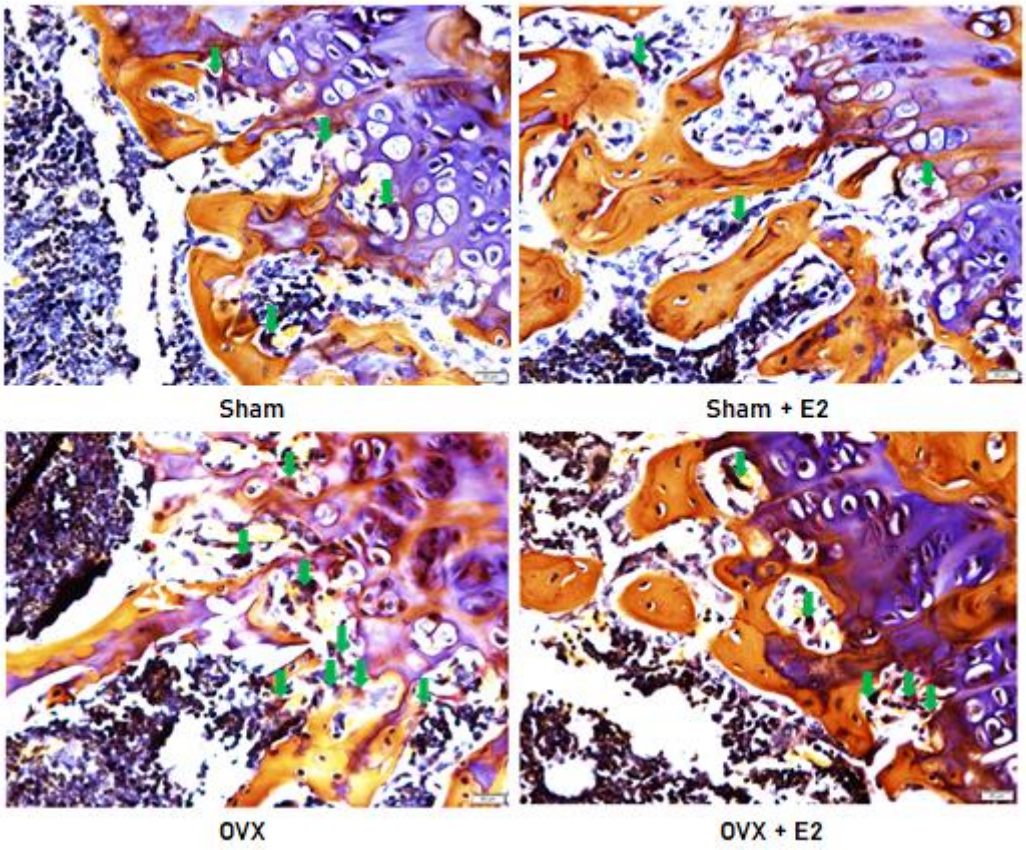
Sham
Sham + E2
OVX
OVX + E2

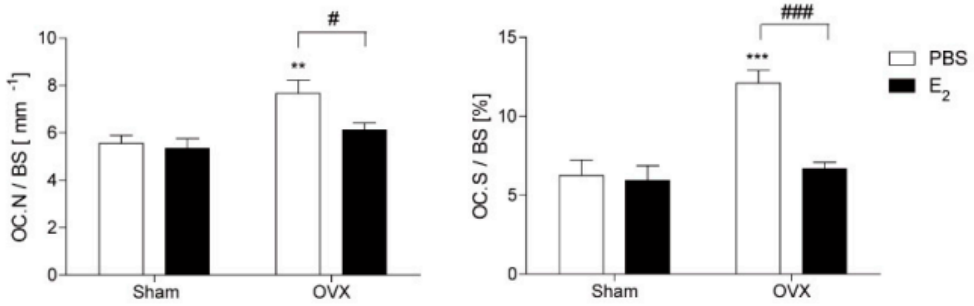
OC.N / BS [mm -1]
#
**
Sham
OVX
OC.S / BS [%]
###
***
PBS
E2

B

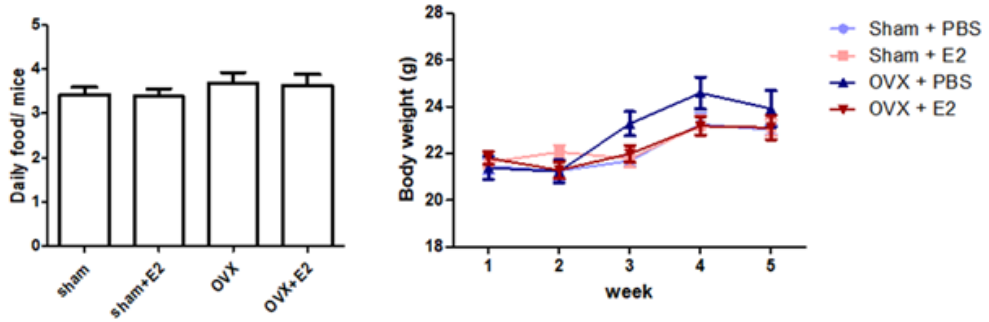
Daily food/ mice
sham
sham+E2
OVX
OVX+E2
Body weight (g)
week
Sham + PBS
Sham + E2
OVX + PBS
OVX + E2

Fig. 1. Estrogen decreases number and size of OCs during bone loss in OVX mice.

Ten-week-old female mice were subjected to sham operation (n = 10) or OVX (n = 12), and E_2 (0.1 mg/kg) or vehicle was injected (5 mice for sham, 6 mice for OVX) intraperitoneally daily for 4 weeks.To assess number and area of osteoclasts *in vivo*, mouse femora were excised, cleaned with a soft tissue, and decalcified in EDTA. Representative histological sections of the distal femoral metaphysis of mice from each of the 4 groups were stained for TRAP to identify OCs (indicated by arrows) to calculate OC surface area divided by total bone surface area (OC.S/BS) and OC number divided by total bone surface (OC.N/BS). Scale bar in the representative photos: 50 μm. Inset shows higher magnification (Scale bar: 20 μm Two-way ANOVA, followed by Bonferroni posttests was used to compare the effect of E_2 (OC.N/BS; $p < 0.05$, OC.S/BS; $p < 0.001$), the effect of surgery (serum CTX-1; $p < 0.05$, OC.N/BS; $p < 0.01$, OC.S/BS; $p < 0.001$) and interactions (OC.S/BS; $p < 0.01$) for body weight and food intake (A, B).

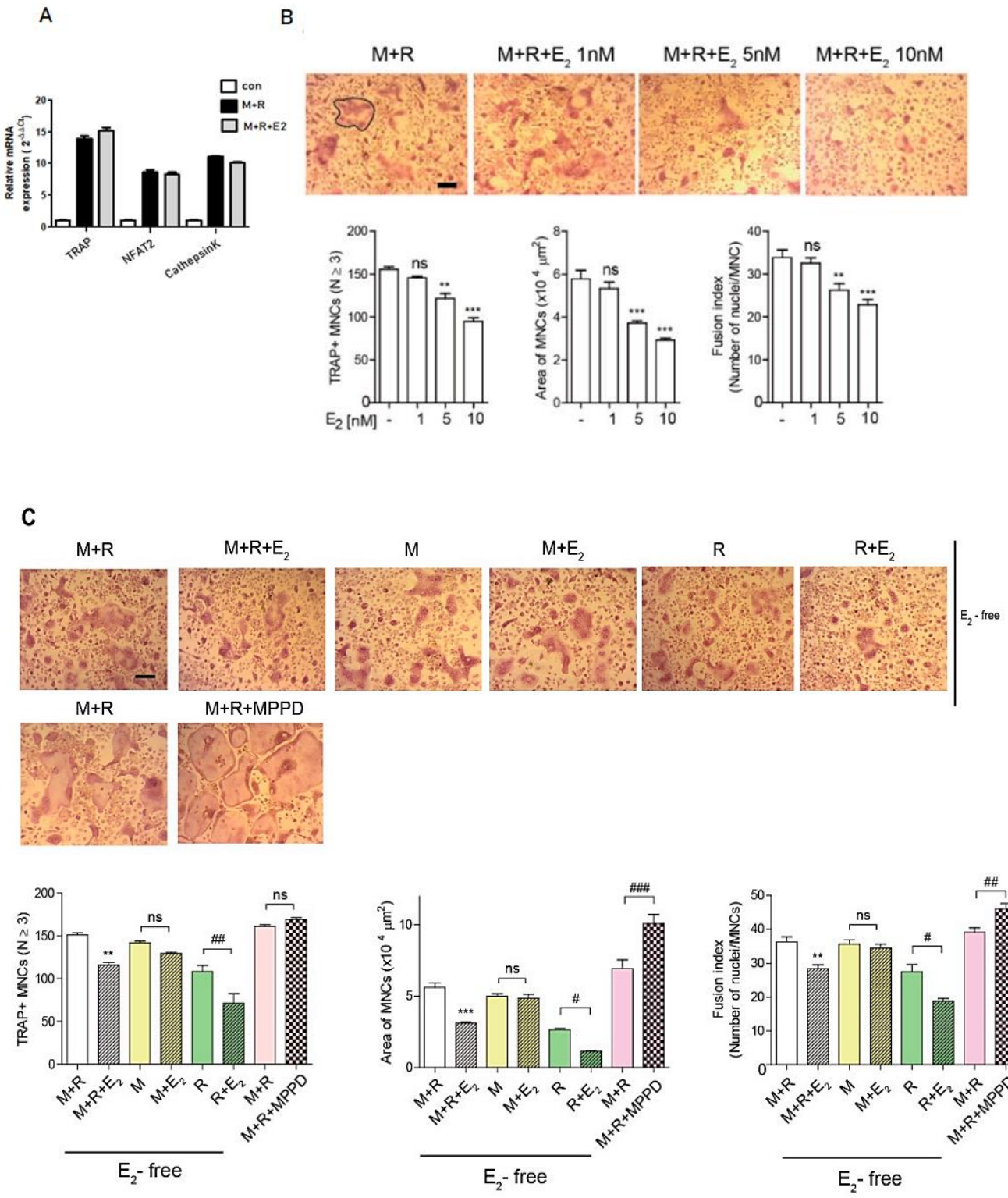
A
B
C
con
M+R
M+R+E2
Relative mRNA expression ($2^{-\Delta\Delta Ct}$)
TRAP
NFAT2
CathepsinK
M+R
M+R+E_2 1nM
M+R+E_2 5nM
M+R+E_2 10nM
TRAP+ MNCs (N ≥ 3)
Area of MNCs (x10^4 μm^2)
Fusion index (Number of nuclei/MNC)
E_2 [nM] - 1 5 10
ns
**
***
M+R
M+R+E_2
M
M+E_2
R
R+E_2
E_2 - free
M+R
M+R+MPPD
TRAP+ MNCs (N ≥ 3)
Area of MNCs (x10^4 μm^2)
Fusion index (Number of nuclei/MNCs)
##
###
#
E_2- free

Fig. 2. Estrogen inhibits number and size of OCs during osteoclast differentiation *in vitro*.

BMMs cultured with M-CSF (30 ng/ml) and RANKL (40 ng/ml) in the presence of E_2 (5 nM) for 48 h were harvested and subjected to RNA extraction and qPCR. The expression level of genes is normalized to cells before treatment of RANKL (A). BMMs treated with M-CSF (30 ng/ml) and RANKL (40 ng/ml) for 55 h, incubated more with E_2 (1 nM, 5 nM, 10 nM) or MPPD (2 μM) was added for another 16 h upon M-CSF and/or RANKL to determine TRAP-positive MNCs (B, C). In case of E_2 treatment, BMMs were cultured in α-MEM without phenol red containing 10% charcoal-treated FBS. After TRAP staining, the TRAP positive cells counted and 70≥ TRAP-positive MNCs randomly selected to measure the area and fusion index (B, C). The fusion index is presented as average number of nuclei per TRAP-positive MNC. Representative photos are shown with scale bar: 100μm. ** $P < 0.01$; *** $P < 0.001$ compared with vehicle group. # $p < 0.05$; ## $p < 0.01$; ### $p < 0.001$ compared with each corresponding control. Similar results were obtained in three independent experiments [Antioxidants 2021, 10, 619. https://doi.org/10.3390/antiox10040619].

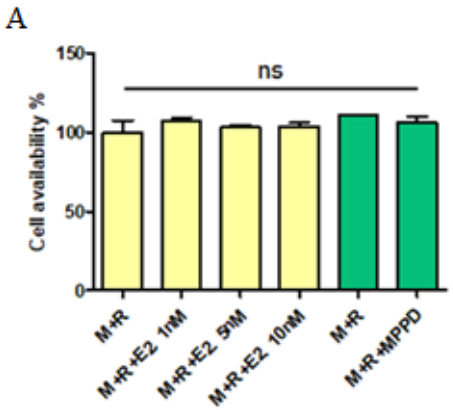
A
Cell availability %
150
100
50
0
ns
M+R
M+R+E2 1nM
M+R+E2 5nM
M+R+E2 10nM
M+R
M+R+MPPD

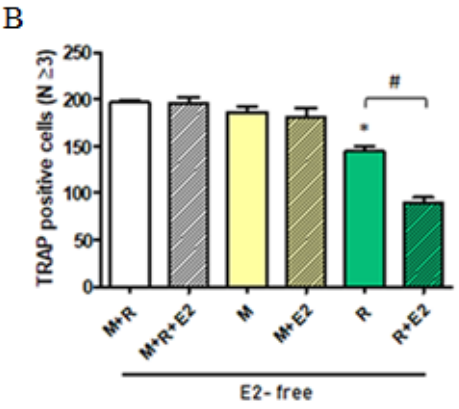
B
TRAP positive cells (N ≥3)
250
200
150
100
50
0
#
*
M+R
M+R+E2
M
M+E2
R
R+E2
E2- free

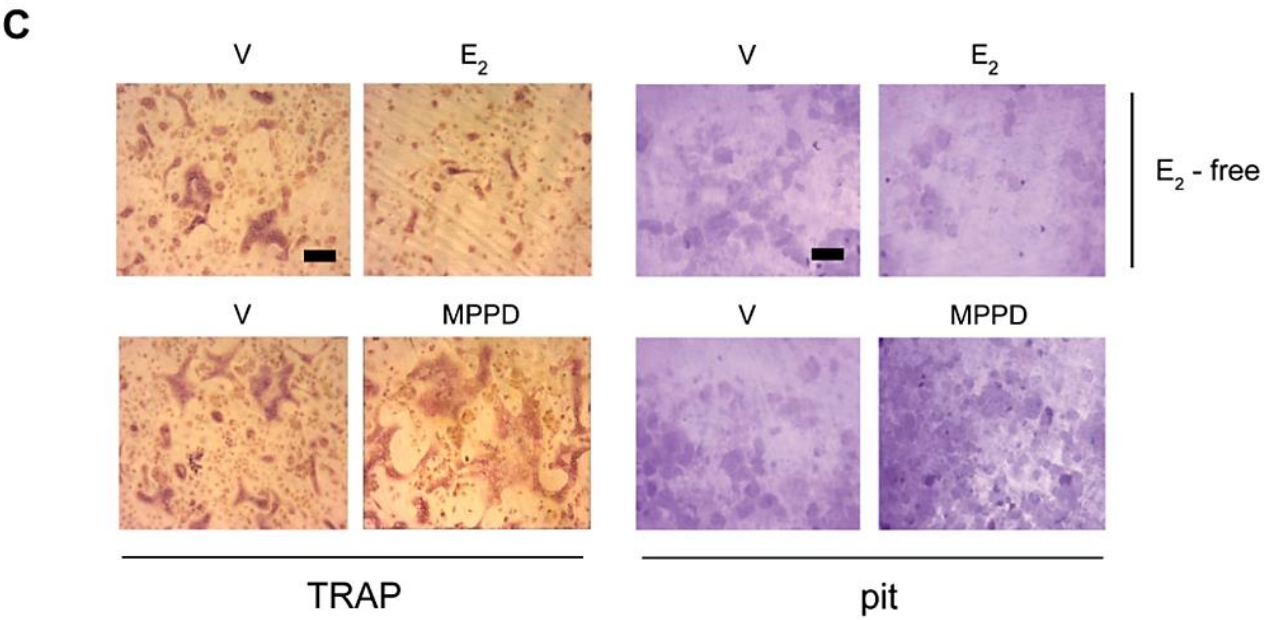
C
V
E2
V
E2
E2 - free
V
MPPD
V
MPPD
TRAP
pit

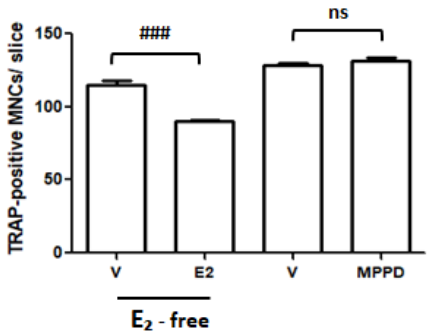
TRAP-positive MNCs/ slice
150
100
50
0
###
ns
V
E2
V
MPPD
E2 - free

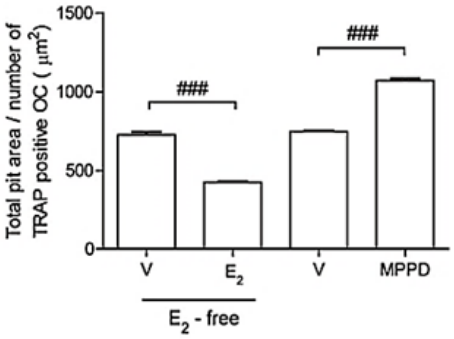
Total pit area / number of TRAP positive OC (μm2)
1500
1000
500
0
###
###
V
E2
V
MPPD
E2 - free

Fig. 3. E_2 inhibits Bone resorption activity via disrupting RANKL-induced cytoskeletal reorganization

To check the cell viability, MTT assay is performed in presence of different concentration of E2 upon RANKL stimulation (A). Mature osteoclasts are treated further in presence of different cytokines (M-CSF and RANKL) with or without E2 to identify the cytokine signaling as target for E2 (B). Mature OCs were incubated more on dentine slices with M-CSF and RANKL in the presence or absence of E_2 (5 nM) or MPPD (2 μM) for 3 days. After TRAP staining, the cells were removed via sonification and the slices were stained with toluidine blue. Representative photos of TRAP-positive OCs and resorption pits are shown in scale bar: 100μm. Total pit area/number of TRAP-positive OCs was calculated (C) [Antioxidants 2021, 10, 619. https://doi.org/10.3390/antiox10040619]. * $p < 0.05$; ** $p < 0.01$; *** $p < 0.001$ compared with control. # $p < 0.05$; ## $p < 0.01$; ### $p < 0.001$ compared with each corresponding control. Similar results were obtained in three independent experiments.

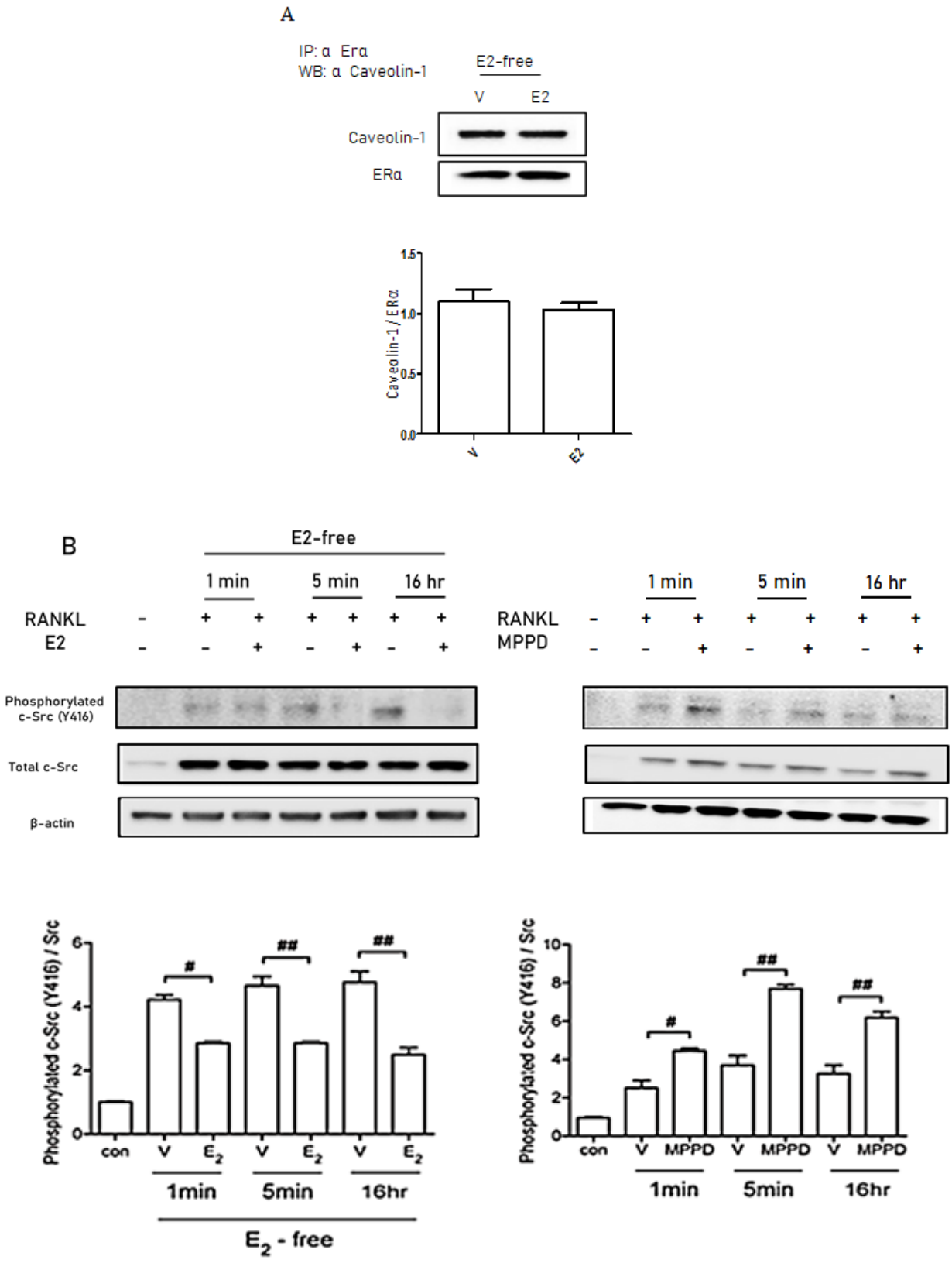
A
IP: α Erα
WB: α Caveolin-1
E2-free
V
E2
Caveolin-1
ERα
Caveolin-1 / ERα
1.5
1.0
0.5
0.0
V
E2
B
E2-free
1 min
5 min
16 hr
RANKL
E2
MPPD
Phosphorylated c-Src (Y416)
Total c-Src
β-actin
Phosphorylated c-Src (Y416) / Src
con
V
E2
MPPD
1min
5min
16hr
E2 - free

Fig. 4. E_2 transmits signaling via ERα, resulting in disrupted c-Src activation in a non-genomic manner.

BMMs were cultured with M-CSF (30 ng/ml) and RANKL (40 ng/ml) for 55 hours, after washing incubated more with RANKL (50 ng/ml) with or without E_2 (5 nM) and MPPD (2 μM) for the indicated time. For E_2 treatment, BMMs were cultured in α-MEM without phenol red containing 10% charcoal-treated FBS (E_2-free). Cell lysate was immunoblotted for phosphorylated c-Src (Y416) normalized with total Src and β-actin (A). Cell lysates were subjected to co-immunoprecipitation with specific antibodies against ERα and immunobloted with antibody against Caveolin-1. # $p < 0.05$; ## $p < 0.01$ compared with each corresponding control. Similar results were obtained in three independent experiments.

A

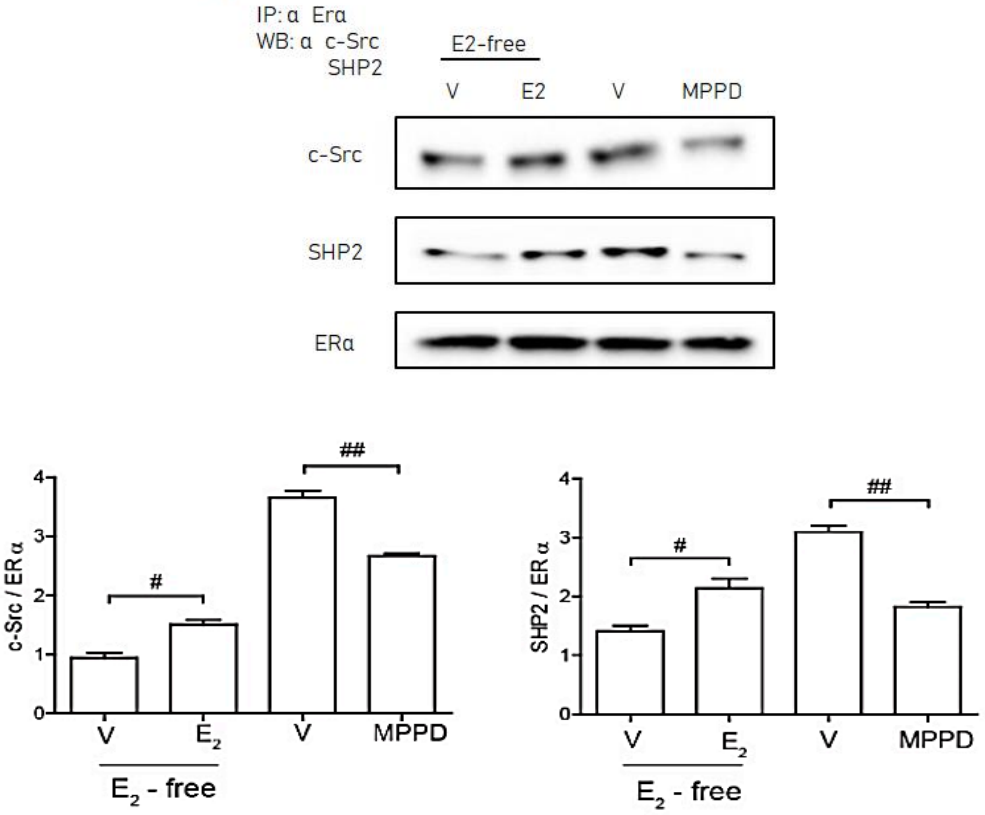
IP: α Erα
WB: α c-Src
SHP2
E2-free
V
E2
V
MPPD
c-Src
SHP2
ERα
c-Src / ER α
SHP2 / ER α
#
##
V
E2
MPPD
E2 - free

B

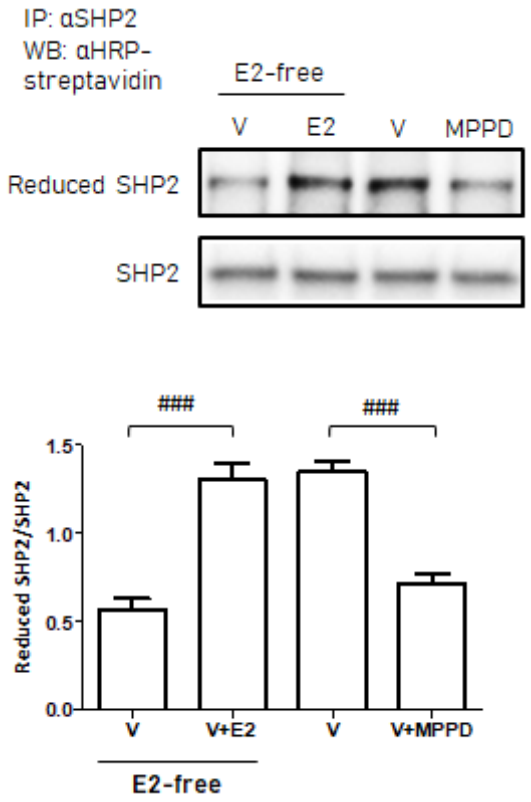
IP: αSHP2
WB: αHRP-streptavidin
E2-free
V
E2
V
MPPD
Reduced SHP2
SHP2
Reduced SHP2/SHP2
###
V
V+E2
V+MPPD
E2-free

C

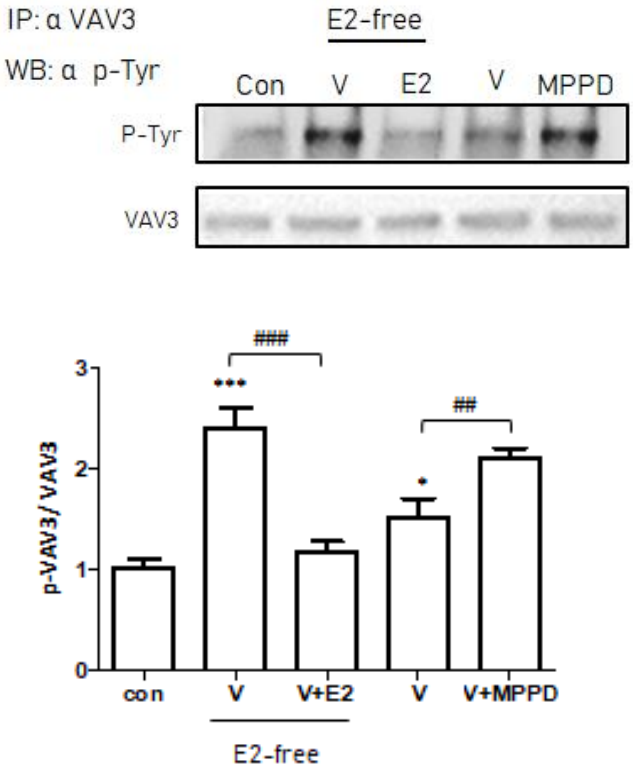
IP: α VAV3
WB: α p-Tyr
E2-free
Con
V
E2
V
MPPD
P-Tyr
VAV3
p-VAV3/ VAV3
###
***
##
*
con
V
V+E2
V
V+MPPD
E2-free

Fig. 5. E_2 decreases c-Src activation by forming an ERα/c-Src/SHP2 complex

BMMs were cultured with M-CSF (30 ng/ml) and RANKL (40 ng/ml) for 55 hours, after washing, incubated further with RANKL (50 ng/ml) in the absence or presence of E_2 (5 nM) or MPPD (2 μM) for the indicated time. In case of E_2 treatment, BMMs were cultured in α-MEM without phenol red containing 10% charcoal-treated FBS (E_2-free). Cell lysates were prepared for co-immunoprecipitation with specific antibodies to Erα and VAV3, then subjected to immunoblotting as indicated (A, C). To check the reduced form of SHP2, the cell lysate were subjected to immunoprecipiotation with anti-SHP2 after labeling with BIAM and then were immunobloted with HRP-streptavidin (B). * $p < 0.05$; ** $p < 0.01$; *** $p < 0.001$ compared with control. # $p < 0.05$; ## $p < 0.01$ compared with each corresponding control. Similar results were obtained in three independent experiments.

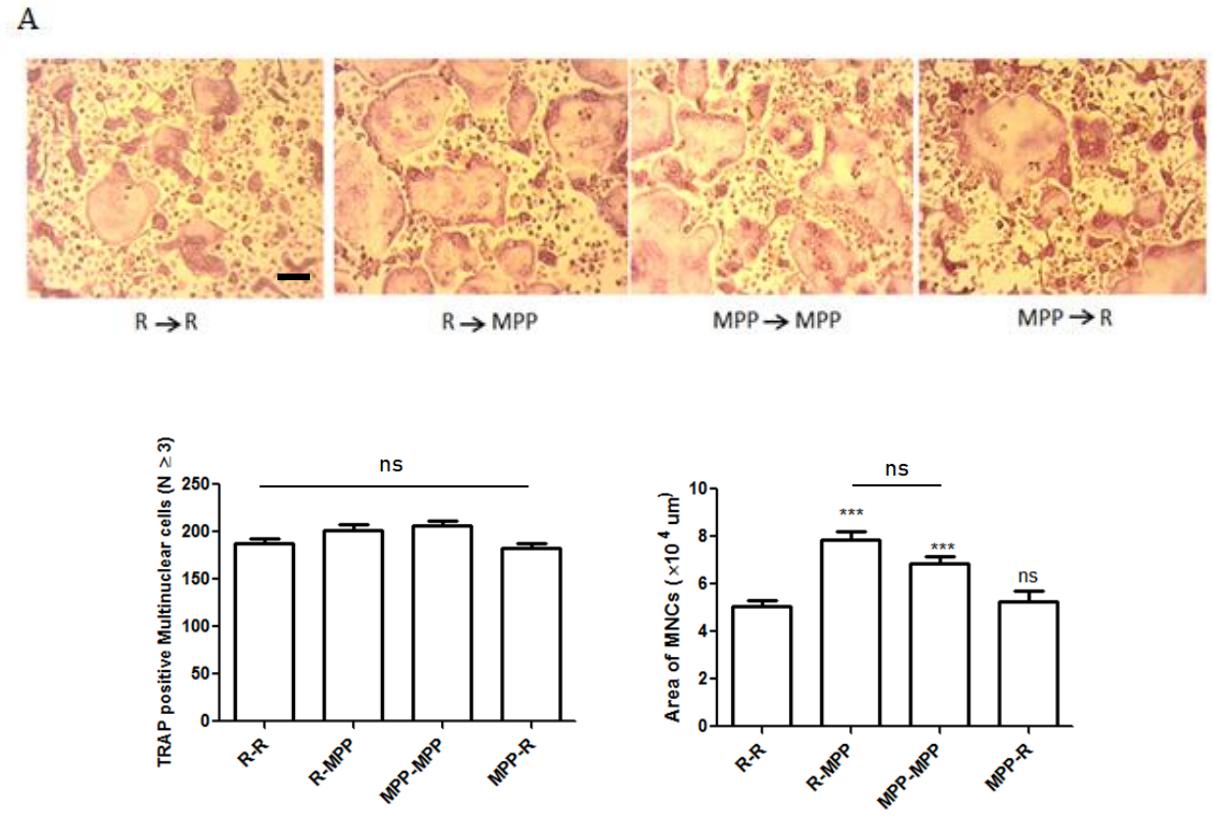
A
R → R
R → MPP
MPP → MPP
MPP → R
TRAP positive Multinuclear cells (N ≥ 3)
ns
250
200
150
100
50
0
R-R
R-MPP
MPP-MPP
MPP-R
Area of MNCs (×10 4 um)
ns
***
***
ns
10
8
6
4
2
0
R-R
R-MPP
MPP-MPP
MPP-R

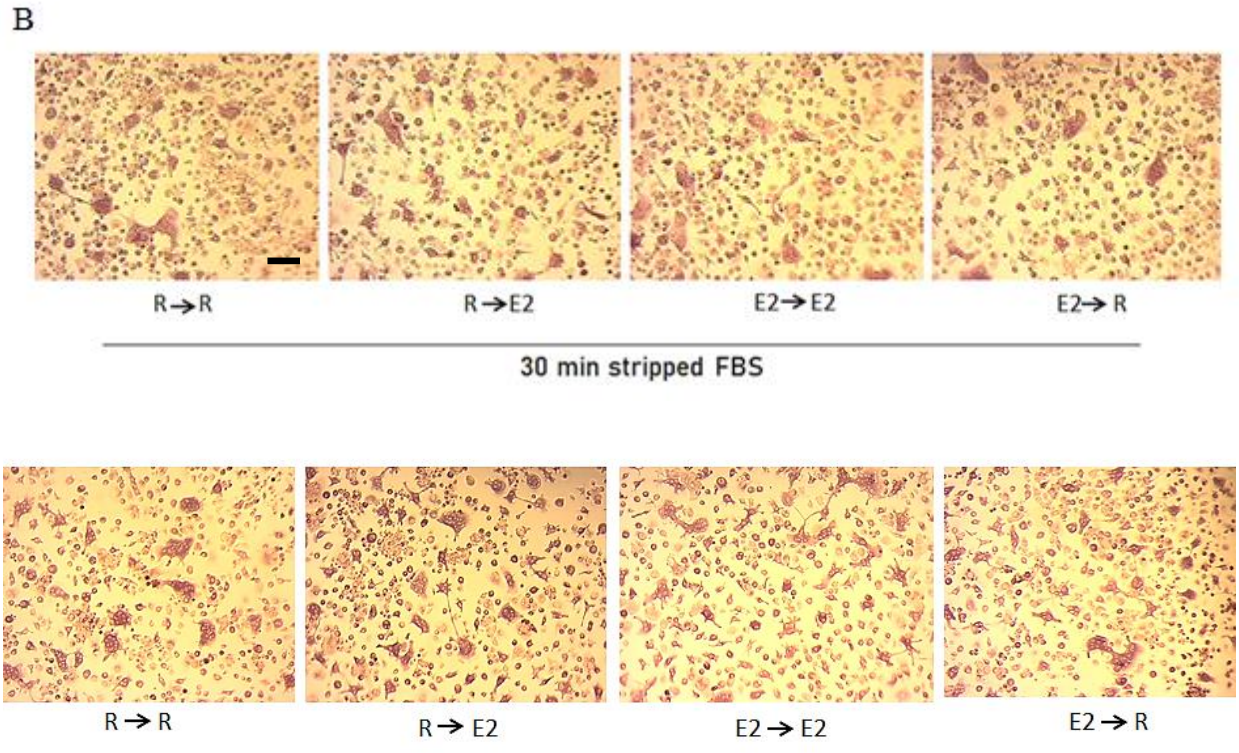
B
R → R
R → E2
E2 → E2
E2 → R
30 min stripped FBS
R → R
R → E2
E2 → E2
E2 → R
4hr stripped FBS

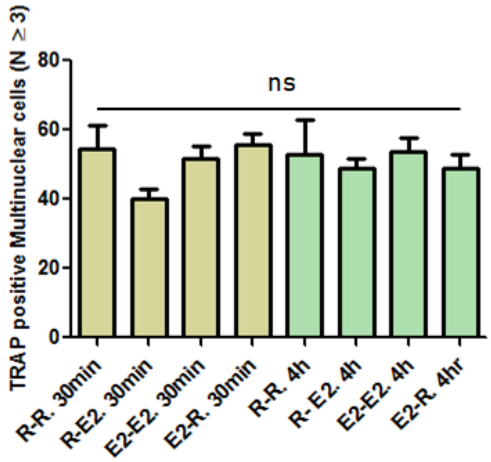
TRAP positive Multinuclear cells (N ≥ 3)
80
60
40
20
0
ns
R-R. 30min
R-E2. 30min
E2-E2. 30min
E2-R. 30min
R-R. 4h
R-E2. 4h
E2-E2. 4h
E2-R. 4hr

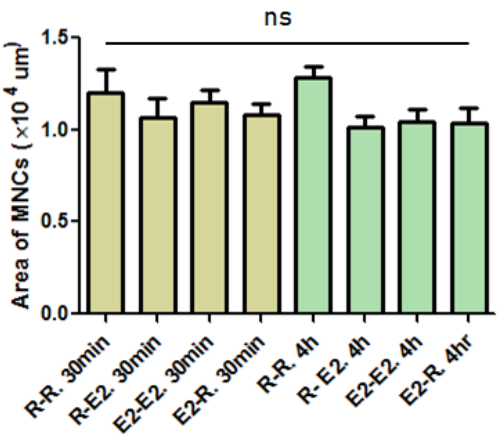
ns
Area of MNCs (×10 4 um)
1.5
1.0
0.5
0.0
R-R. 30min
R-E2. 30min
E2-E2. 30min
E2-R. 30min
R-R. 4h
R-E2. 4h
E2-E2. 4h
E2-R. 4hr

Supplementary Figure 1

Optimized timing for treatment of MPPD and stripping the FBS for E2 treatment

To investigate the time for MPPD treatment, the BMM cells were treated with MPPD (2μM) in defined conditions (A). To assess the time for stripping the FBS with charcoal, incubation of FBS was done in both 30 min and 4 hr and the BMM cells incubated using both 30 min and 4hr stripped FBS and differentiated to osteoclast (B).

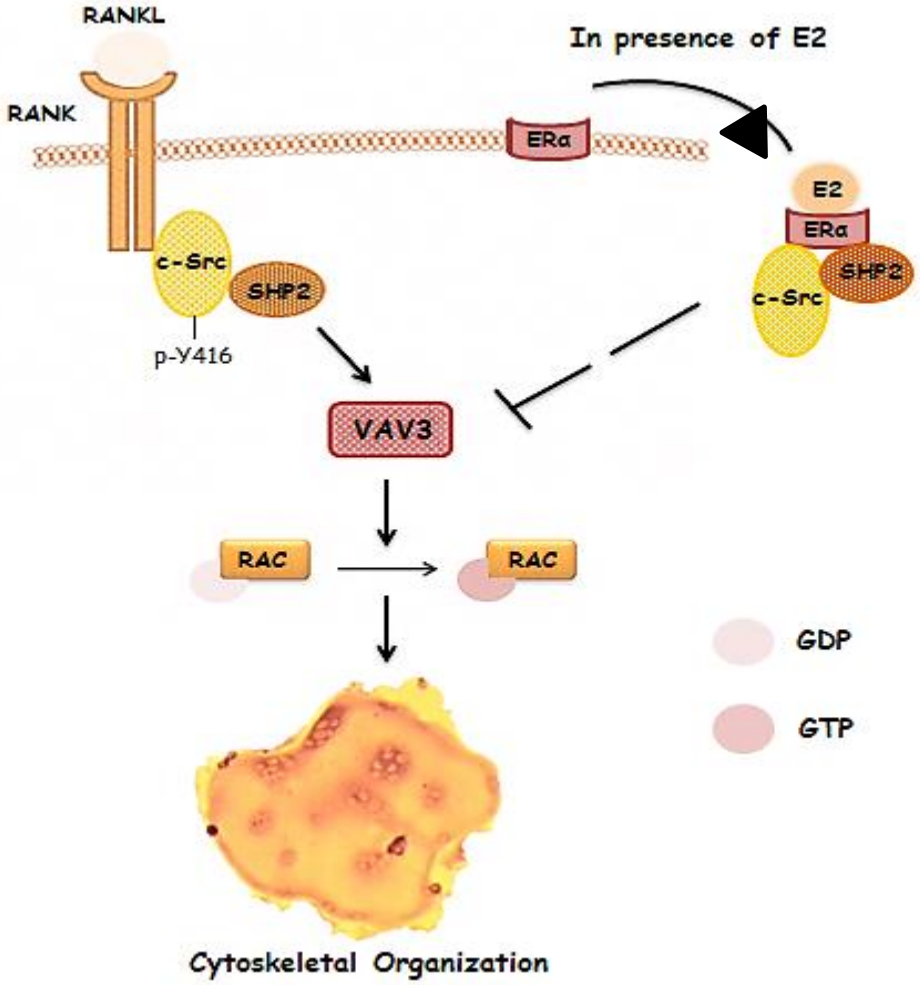
RANKL
RANK
In presence of E2
ERα
E2
ERα
SHP2
c-Src
c-Src
SHP2
p-Y416
VAV3
RAC
RAC
GDP
GTP
Cytoskeletal Organization

References used for ABSTRACT figure:

1. Izawa, T.; Zou, W.; Chappel, J. C.; Ashley, J. W.; Feng, Xu.; Teitelbauma, S. L. c-Src Links a RANK/ v 3 Integrin Complex to the Osteoclast Cytoskeleton. Molecular and cellular Biology. 2012, 32 (14), 2943- 2953.
2. Zou, W.; Kitaura, H.; Reeve, J.; Long, F.; Tybulewicz, V. L. J.; Shattil, S. J.; Ginsberg, M. H.; Ross, F. P.; Teitelbaum, S. L. Syk, c-Src, the αvβ3 integrin, and ITAM immunoreceptors, in concert, regulate osteoclastic bone resorption. The Journal of Cell Biology. 2007, 176 (6), 877–888.